

30. CRETACEOUS FORAMINIFERAL BIO-ISOTOPE STRATIGRAPHY OF HOLE 967E AND PALEOGENE PLANKTONIC FORAMINIFERAL BIOSTRATIGRAPHY OF HOLE 966F, EASTERN MEDITERRANEAN¹

Isabella Premoli Silva,² Silvia Spezzaferri,³ and Antonio D'Angelantonio²

ABSTRACT

During Ocean Drilling Program Leg 160, pelagic middle Eocene sediments were recovered from Hole 966F. Cretaceous and pelagic lower Oligocene sediments were recovered from Hole 967E. Both sites are located on the Eratosthenes Seamount, on the top and lower slope, respectively. The Cretaceous succession consists of pelagic sediments that overlie carbonate platform sediments. The deposition of carbonate platform sediments occurred in a shallow-water, lagoonal environment and ended in the late Aptian. Cretaceous pelagic sedimentation may have started in the Cenomanian(?) and continued up through the Maastrichtian. Despite poor recovery, a hiatus spanning the middle to late *Helvetoglobotruncana helvetica* Zone and the *Marginotruncana sigali* Zone is probably present in the Turonian, as inferred by the estimated very low sedimentation rates, and another hiatus is hypothesized between shallow-water carbonates and the overlying pelagic sequence, probably spanning the entire Albian and part of the Cenomanian. Another major hiatus was detected in Hole 967E where lower Oligocene sediments rest on upper Maastrichtian deposits. The planktonic assemblages reworked within the lower Oligocene sediments, however, indicate that sedimentation was originally more continuous on the seamount, and that several intervals were removed by downslope transport. Stable isotope stratigraphy (oxygen and carbon) tentatively allows comparison of the Cretaceous isotope record of Hole 967E with continuous and well-dated land sections in central Italy.

INTRODUCTION

Drilling on the Eratosthenes Seamount during Ocean Drilling Program (ODP) Leg 160 provided the first record of pre-Miocene pelagic and shallow-water sediments from the Eastern Mediterranean since the first Deep Sea Drilling Project cruise (Leg 13) in 1970. Pre-Miocene sediments were recovered in two holes from the top of the seamount (Hole 966F) and the lower slope (Hole 967E), along a transect drilled across the Eratosthenes Seamount to the Cyprus margin (Fig. 1). In Hole 966F a relatively undisturbed and clean pelagic chalk of middle Eocene age was recovered. Hole 967E penetrated deeper into the seamount, recovering a very mixed Paleogene pelagic sequence and a 400-m-thick chalk unit of Late Cretaceous age resting on a shallow-water carbonate platform belonging to the upper part of the seamount (Emeis, Robertson, Richter, et al., 1996).

This paper documents the planktonic foraminiferal distribution within the pelagic units from both Holes 966F and 967E and the distribution of shallow-water organisms and facies from the carbonate platform unit of Hole 967E.

MATERIALS AND METHODS

Sample spacing was guided by the preliminary biostratigraphic investigations, core recovery, and lithology. It resulted in a variable sample density for the different intervals. Samples were taken at every change in lithology in the lower cores with very poor recovery. In the overlying chalk unit, samples were taken on the average of every 50 to 100 cm. Micropaleontological studies were performed in thin section from the harder lithotypes in Cores 160-967E-50R up to 29R. From Core 160-967E-30R up to Core 160-967E-8R softer lithotypes

allowed disaggregation. Samples of about 5 to 10 cm³ were soaked in distilled water and washed under running water through 40–150 µm, 150–250 µm, and >250 µm sieves. The three size fractions obtained were then dried at room temperature.

Abundance of single foraminiferal species and groups and other organic and inorganic components relative to the total biogenic content were estimated for both thin sections and washed residues. Five categories were distinguished and plotted in the range charts as follows (Tables 1–3): VR = very rare (1–2 specimens); R = rare (2–5 specimens); F = few (5–10); C = common (10–30 specimens); A = abundant (>50% of the total fauna and/or biogenic content); AA = very abundant; AAA = extremely abundant (dominant).

Presence of organic and inorganic components is indicated as follows: sp = spicules; ph = phosphatic remains; fish = fish teeth; og = organic matter; I = inoceramids; E = echinoderms; O = ostracods; qtz = quartz; ox = oxide; gl = glauconite; v = volcanics; ch = chert; red = brilliant red grains of unknown origin.

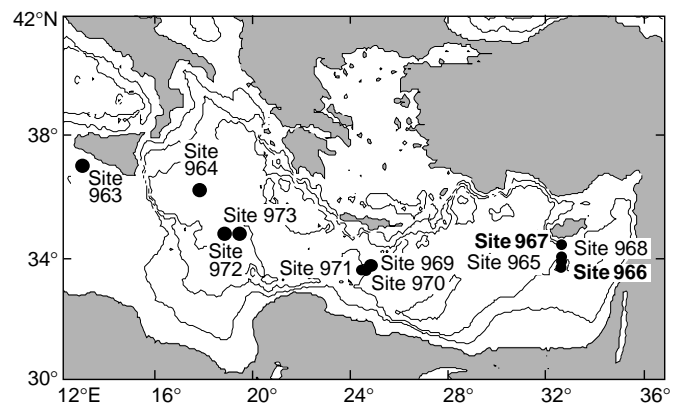


Figure 1. Location map of Sites 963 through 973, drilled during Leg 160. Sites 966 and 967 (this study) are shown in bold (after Emeis, Robertson, Richter, et al., 1996).

¹Robertson, A.H.F., Emeis, K.-C., Richter, C., and Camerlenghi, A. (Eds.), 1998. *Proc. ODP, Sci. Results*, 160: College Station, TX (Ocean Drilling Program).

²Dipartimento di Scienze della Terra, Università di Milano, Via Mangiagalli 34, 20133, Milano, Italy. micro@imucca.csi.unimi.it

³ETH-Zentrum, Geologisches Institut, Sonneggstrasse 5, 8092, Zurich, Switzerland.

Oxygen and carbon isotopes were measured on 67 bulk sediment samples, using a PRISM mass spectrometer at the ETH-Zurich. The isotope data, corrected following the procedure of Craig (1957) modified for a triple collector and relative to the international PeeDee belemnite (PDB) standard, are given in Table 5.

BIOSTRATIGRAPHY

The age determinations of the Cretaceous and Paleogene pelagic sequences encountered in this study are based on planktonic foraminiferal zonal schemes proposed by Robaszynski et al. (1990, 1993), Premoli Silva and Sliter (1994), Robaszynski and Caron (1995), and Erba et al. (1995) for the Cretaceous, and Blow (1969, 1979) for the Paleogene.

Generic attribution and identification of planktonic foraminiferal zones follow Robaszynski et al. (1979, 1984, 1990, 1993), Caron (1985), Nederbragt (1990), Premoli Silva and Sliter (1994) for the Cretaceous taxa; Boersma and Premoli Silva (1983), Toumarkine and Luterbacher (1985), Boersma et al. (1987), Premoli Silva and Boersma (1988, 1989), Hemleben et al. (1991), Olsson et al. (1992), and Spezzaferri (1994) for the Paleogene taxa. In addition, De Castro (1966), Fourcade (1980), and Arnaud Vanneau and Premoli Silva (1995) were considered for identifying and interpreting shallow-water facies and larger foraminifers from Unit IV. Some Cretaceous planktonic and shallow-water taxa are illustrated in Plates 1 through 4.

Hole 966F

Hole 966F is located on the northern edge of the plateau area of the Eratosthenes Seamount ($33^{\circ}47.858'N$, $32^{\circ}42.093'E$, water depth 922.9 m, penetration 356 m). The hole was drilled to 59 m. Rotary Core Barrel (RCB) Cores 160-966F-1R through 31R were taken from 0 to 356 mbsf, with 297 m cored and 65.85 m recovered (recovery rate 22.1%). Eocene sediments were encountered at about 300 mbsf (Section 160-966F-26R-1), below a shallow-water carbonate sequence attributed to the Miocene, based on the presence of large benthic foraminiferal assemblages (Emeis, Robertson, Richter, et al., 1996). These rich assemblages contain numerous lepidocyctinids and miogypsids. Their poor preservation and cuts, however, prevented identification at species level and resulted in a less precise age attribution.

The Eocene planktonic foraminiferal assemblages from Hole 966F are moderately abundant and generally poorly preserved (Table 1). They consist of planktonic assemblages typical of middle Eocene Zones P10–P12, which include *Acarinina bullbrookii*, *A. pentacamerata*, *A. matthewsae*, *A. pseudotopilensis*, *A. rugosoaculeata*, *Globanomalina pseudoscitula*, *Igorina broedermannii*, *Turborotalia pomeroli*, *T. griffinae*, *T. praecentralis*, and *T. pseudomayeri*. Minor components include *Turborotalia cerroazulensis*, *T. pseudoampliapertura*, *Subbotina praeturrilitina*, *Dentoglobigerina galavisi*, *Zeaglobigerina ampliapertura*, *Morozovella aragonensis*, *M. lehneri*, and the *Subbotina angiporoidea* group.

Reworking of older specimens ranges from very rare to rare/common. It consists of rare specimens of early to mid-Paleocene and early Eocene species such as *Praemurica uncinata*, *Morozovella conicotruncata*, *M. gracilis*, *M. subbotinae*, and *Acarinina nitida*. In Sample 160-966F-28R-3, 74–76 cm, reworking consists of only a few Cretaceous forms such as hedbergellids and *Pseudotextularia* sp.

Hole 967E

Hole 967E is located on the lower northern slope of the Eratosthenes Seamount ($34^{\circ}04.106'N$, $32^{\circ}43.525'E$, water depth 3164.3 m, penetration 600.3 m) (Emeis, Robertson, Richter, et al., 1996). The hole was drilled to 109.5 mbsf. RCB Cores 160-967E-1R

through 51R were taken from 109.5 to 600.3 mbsf, with 598.35 m cored and 72.3 m recovered (recovery rate 14.8%). Paleogene sediments were encountered between 130 and 177 mbsf; they overlie a pelagic Cretaceous sedimentary sequence that extends down to 430 mbsf (Figs. 2, 3). The sediments below the pelagic interval down to a total depth of 600.3 m consist of shallow-water carbonates deposited in a lagoonal environment.

Shallow-Water Carbonate Facies

Several samples were studied in thin section from Core 160-967E-50R to 34R (Table 2). This succession spans the interval from the upper part of the carbonate platform through the base of the pelagic sequence.

The shallow-water facies of Unit IV overall contain very poor assemblages, mainly indicating deposition in the inner part of a restricted lagoon that rarely experienced good communication with the open ocean (Arnaud Vanneau and Premoli Silva, 1995). As shown in Table 2, ostracods and *Istriloculina* are the only biogenic components in most facies dominated by micrite due to bacterial activity and/or pellets. Scattered richer assemblages contain miliolids, nezzazzatids, and, rarely, small agglutinated foraminifers. Calcareous algae were rarely recorded.

Few age-diagnostic larger foraminifers, mainly *Archaealveolina reicheli*, were encountered in Cores 160-967E-41R, 37R, and 35R. A few specimens of *A. reicheli* were found associated with *Cuneolina* sp. in the latter core (160-967E-35R). According to De Castro (1966) and Fourcade (1980), *A. reicheli* is stratigraphically confined to the upper Aptian. A fragment of a cuneolinid was also found in Core 160-967E-34R associated with the oldest, long-ranging, planktonic foraminifers recorded from Hole 967E. According to the lithologic description (Emeis, Robertson, Richter, et al., 1996), the samples studied from Cores 160-967E-35R and 34R are resedimented calcarenites interbedded within nannofossil chalk. Thus, the presence of *A. reicheli* in Core 160-967E-35R suggests that the shallow-water carbonate deposition ended in the late Aptian.

Cretaceous Planktonic Foraminifers

Planktonic foraminiferal assemblages from pelagic Unit III, overlying the shallow-water carbonates, are unevenly distributed throughout (Tables 2, 3). Size-sorting is very clearly shown by the variable abundance of large-sized planktonic species (>250 μ m) and benthic foraminifers. As a result of sorting, zonal markers are rare throughout. Fine fractions (<150 μ m) are dominated by fragmented larger sized or juvenile planktonic specimens, small-sized plankton, and small, mostly broken benthic foraminifers. Reworking is evident only in the lower part of the unit. These features imply that sedimentation occurred under a rather high energy environment.

In the lower part of the unit (Cores 160-967E-33R through 31R), planktonic assemblages are dominated by calcispheres and pithomelids (Table 2); their abundance dilutes the planktonic foraminifers to the point that age-diagnostic species are rare and poorly recognizable. In particular, the age of Cores 160-967E-35R through 32R could not be specified with certainty (Fig. 2). Two specimens of a possible *Rotalipora* were found in Samples 160-967E-33R-1, 7–10 cm, and 160-967E-32R-1, 56–60 cm, associated with a few fragments of double keeled taxa and a few specimens of *Favusella washitensis*, respectively.

The double keeled fragments in Sample 160-967E-33R-1, 7–10 cm, although not positively identified, may belong to either the dicarinellids or marginotruncanids. Given the first case (dicarinellids), the age of both samples (160-967E-33R-1, 7–10 cm, and 32R-1, 56–60 cm) would be “mid” to late Cenomanian based on the distribution of *F. washitensis*. Conversely, if the double keeled specimens represent marginotruncanids, both samples cannot be older than the middle part of the *Helvetoglobotruncana helvetica* Zone of Turonian age,

Table 1. Distribution of middle Eocene planktonic foraminifers in Hole 966F.

Core, section, interval (cm)	Depth (mbsf)	Zones	A. bullbrookii	G. carcosellensis	I. bredoermmanni	S. inaequispira	A. penitacamerata	G. micra	P. pseudoscitulus	G. index	A. rugosoculaea	A. angiporoidea minima	A. primitiva	T. bowieri	S. utilisindex	Chilogumbelina sp.	A. angiporoidea	M. aragonensis	T. pracentralis	D. galivisi	T. gemma	S. hornbrookii	T. griffinae	C. unicavus	A. matthewsae	Hankenina sp.	G. subconglobata	
160-966F-																												
26R-2, 1-4	299.1		X	—	—	—	X	—	—	—	—	—	—	—	—	—	—	—	—	—	—	—	—	—	—	—	—	
26R-4, 41-44	302.3		—	—	—	—	X	—	—	—	—	—	—	—	—	—	—	—	—	—	—	—	—	—	—	—	—	
27R-1, 74-77	308.6		X	—	—	—	X	X	X	X	X	X	X	X	X	X	X	X	X	X	X	X	X	X	X	X	X	
27R-4, 60-64	312.6		—	—	—	—	X	—	X	X	X	X	X	X	X	X	X	X	X	X	X	X	X	X	X	X	X	
27R-6, 25-28	315.1		X	—	—	—	X	—	X	X	X	X	X	X	X	X	X	X	X	X	X	X	X	X	X	X	X	
28R-1, 58-61	318.1	P10-	—	—	—	—	X	—	X	X	X	X	X	X	X	X	X	X	X	X	X	X	X	X	X	X	X	
28R-3, 74-77	320.3	P12	—	—	—	—	X	—	X	X	X	X	X	X	X	X	X	X	X	X	X	X	X	X	X	X	X	
28R-6, 128-131	325.2		X	—	—	—	X	—	X	X	X	X	X	X	X	X	X	X	X	X	X	X	X	X	X	X	X	
29R-1, 73-78	327.8		X	—	—	—	X	X	X	X	X	X	X	X	X	X	X	X	X	X	X	X	X	X	X	X	X	
29R-2, 130-132	329.9		X	X	—	—	X	—	X	X	X	X	X	X	X	X	X	X	X	X	X	X	X	X	X	X	X	
30R-1, 23-27	337.0		—	—	—	—	X	—	—	X	—	—	—	—	—	—	—	—	—	—	—	—	—	—	—	—	—	
30R-3, 94-97	340.7		—	—	X	—	X	—	—	X	—	X	X	X	X	X	X	X	X	X	X	X	X	X	X	X	X	
31R-1, 80-83	347.2		X	X	X	X	X	X	X	X	X	X	X	X	X	X	X	X	X	X	X	X	X	X	X	X	X	
31R-3, 9-12	349.3		X	X	X	X	—	—	—	—	—	—	—	—	—	—	—	—	—	—	—	—	—	—	—	—	—	

Notes: X = present; VR = very rare (1-2 specimens); R = rare (2-5 specimens); C = common (10-30 specimens).

Table 1 (continued).

Core, section, interval (cm)	Depth (mbsf)	Zones	T. pseudomayeri	T. rohri	T. topiensis	T. cerroazulensis	H. longispina	Z. ampliapertura	A. pseudopiliensis	T. pomeroli	"G." venezuelana	S. eocena	P. micra	G. luterbacheri	C. cubensis	G. semiinvoluta	T. pseudoampullipertura	S. linaperta	S. praeturritilina	Reworking
160-966F-			—	—	—	—	—	—	—	—	—	X	—	—	—	—	X	X	X	VR
26R-2, 1-4	299.1		—	—	—	—	—	—	—	—	—	X	—	—	—	—	X	X	—	VR
26R-4, 41-44	302.3		—	—	—	—	—	—	—	—	—	—	—	—	—	—	—	—	—	VR
27R-1, 74-77	308.6		—	—	X	—	—	—	—	—	—	X	X	X	X	X	X	X	X	R
27R-4, 60-64	312.6		—	—	—	—	—	—	—	—	—	X	X	X	X	X	X	X	X	VR
27R-6, 25-28	315.1		—	—	—	—	—	—	—	—	—	X	—	—	—	—	—	—	—	—
28R-1, 58-61	318.1	P10-	X	—	X	—	—	—	—	—	—	X	X	X	X	X	X	X	X	VR
28R-3, 74-77	320.3	P12	X	X	—	—	—	—	—	—	—	X	X	X	X	X	X	X	X	R/C
28R-6, 128-131	325.2		—	—	—	cf	—	—	—	—	—	X	X	X	X	X	X	X	X	—
29R-1, 73-78	327.8		X	X	X	X	—	—	—	—	—	—	—	—	—	—	—	—	—	VR
29R-2, 130-132	329.9		—	—	—	—	—	—	—	—	—	—	—	—	—	—	—	—	—	R
30R-1, 23-27	337.0		—	—	—	—	—	—	—	—	—	—	—	—	—	—	—	—	—	VR
30R-3, 94-97	340.7		—	—	—	—	—	—	—	—	—	—	—	—	—	—	—	—	—	VR
31R-1, 80-83	347.2		—	—	—	—	—	—	—	—	—	—	—	—	—	—	—	—	—	VR
31R-3, 9-12	349.3		—	—	—	—	—	—	—	—	—	—	—	—	—	—	—	—	—	VR

and the rotaliporids and *F. washitensis* must be interpreted as reworked. We believe the presence of possible rotaliporids more likely supports the first interpretation; thus, the initiation of pelagic sedimentation can be dated to the Cenomanian.

One specimen of *H. helvetica* was observed in Sample 160-967E-31R-1, 5-9 cm, associated with common whiteinellids, *Heterohelix*, and very rare questionable dicarinellids. Specimens of marginotruncanids were not positively identified in this sample. Consequently, we assigned Section 160-967E-31R-1 to the lower part of the *H. helvetica* Zone of early Turonian age.

The next identifiable zone is the *Dicarinella concavata* Zone in Interval 160-967E-30R-1, 55-59 cm, of late Turonian age (Robaszynski et al., 1990; Fig. 2; Table 2). Between this and the lower sample (interval 160-967E-31R-1, 5-9 cm), the very poor recovery (<3%) prevents us from documenting the middle to upper part of the *H. helvetica* Zone and the *Marginotruncana sigali* Zone that extends up through the middle Turonian.

From the *D. concavata* Zone upsection to Sample 160-967E-8R-2, 50-52 cm, nine planktonic foraminiferal zones were identified, spanning the interval from the upper Turonian to the upper Maastrichtian, as follows (from bottom to top):

Dicarinella concavata Zone (from 160-967E-30R-1, 55-59 cm, to 160-967E-26R-CC; >45 m)

Diagnosis: Interval from the first occurrence (FO) of the named species to the FO of *Dicarinella asymetrica*.

The zonal marker is common only in two samples from Core 160-967E-29R and was not found in the upper part of the interval (Table 3, back pocket). The planktonic foraminiferal assemblages are mainly composed of small-sized specimens (<250 µm) associated with common to abundant, commonly broken benthic foraminifers. Planktonic foraminifers include common marginotruncanids (only a few identified at species level), whiteinellids, *Heterohelix globulosa*, and *Globigerinelloides ultramicrus*. Less common species with a more scattered record are *Hedbergella flandrina* and *Heterohelix reussi*, plus *Globigerinelloides prairiehillensis* in the upper part. *Dicarinella canaliculata* disappears before the end of the zone. *Contusotruncana fornicate* appears in Sample 160-967E-29R-1, 100-102 cm, and *Sigalia decoratissima carpatica* first occurs in Sample 160-967E-26R-CC. Reworked assemblages from the *H. helvetica* Zone are recorded in Samples 160-967E-30R-1, 15-25 cm; 29R-2, 4-10 cm; and 29R-1, 109-114 cm.

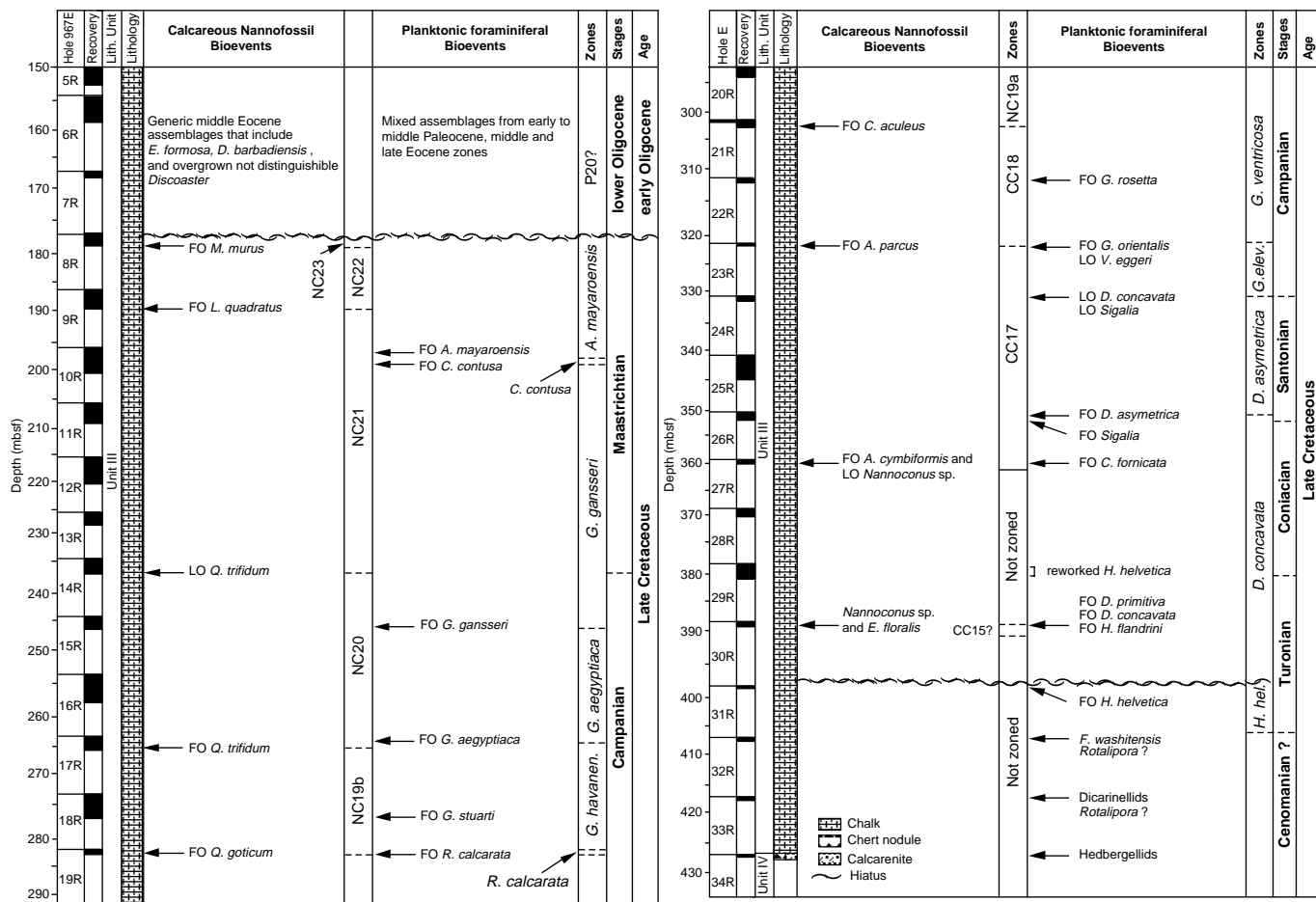


Figure 2. Lithologic log, core recovery, planktonic foraminiferal bioevents, and zone assignment plotted vs. calcareous nannofossil bioevents (after Emeis, Robertson, Richter, et al., 1996) in Hole 967E. Notes: FO = first occurrence, LO = last occurrence. The inferred hiatus between Cores 30R and 31R is arbitrarily placed at the base of Core 30R, and Core 31R was totally attributed to the *H. helvetica* Zone.

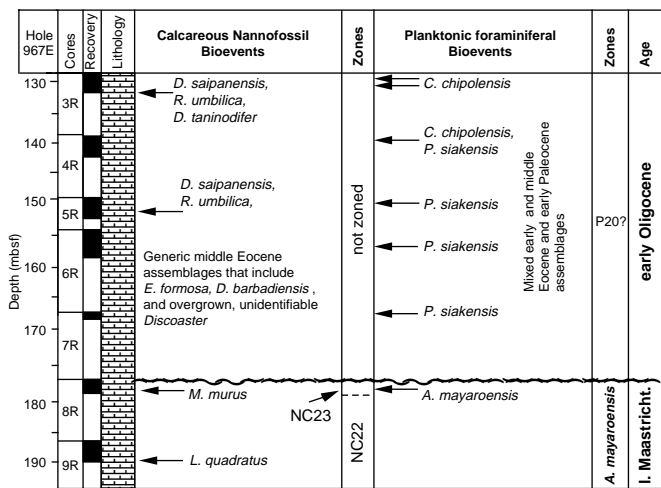


Figure 3. Expanded lithologic log and core recovery plotted vs. occurrence of planktonic foraminifers and zone assignment for the Oligocene succession recovered from Hole 967E. Note: Symbols same as in Figure 2.

Dicarinella asymmetrica Zone (from 160-967E-26R-1, 50–58 cm, to 160-967E-24R; 19.58 m)

Diagnosis: Total range of the zonal marker.

The zonal marker was observed only in the lowermost sample of this zone, but *D. concavata* last occurs in Sample 160-967E-24R-1, 22–23 cm, which was equated to the top of the zone. As in the previous zone, planktonic foraminiferal assemblages are mainly composed of small-sized specimens (<250 µm) associated with common to abundant, often broken benthic foraminifers. The common marginotruncanids rarely could be identified at species level except for rare *Marginotruncana pseudolineiniana*, *M. coronata*, and *M. sinuosa*. Other common species are *G. prairiehillensis*, *Globigerinelloides messinae*, *G. ultramicrus*, *H. globulosa*, *Heterohelix carinata*, *H. striata*, and *Ventilabrella eggeri*. *Sigalia decoratissima carpatica* is scattered, and *Sigalia deflaensis rugocostata* occurs only in the upper part of the interval. Rare *Hedbergella holmdelensis* occurs throughout, whereas rare globotruncanids are recorded only in the middle to upper part of the zone.

Globotruncana elevata Zone (Core 160-967E-23R; 8.82 m)

Diagnosis: Interval from the last occurrence (LO) of *Dicarinella asymmetrica* and *D. concavata* to the FO of *Globotruncana ventricosa*.

Table 2. Distribution of Lower Cretaceous shallow-water components and lower Upper Cretaceous planktonic foraminifers in Hole 967E.

Core, section, interval (cm)	Depth (mbsf)	Benthic foraminifers												Sedimentary features				Hole 967E							
		Ostracods	Benthic foraminifers	Isticulina	Agglutinated foraminifers	Rotaliids	Miliolids	Echinoderms	Brachiopods	<i>Archaeoabeolina richeli</i>	Neazzatids	Crustaceans	Molluscs	Phosphatic remains	Oncoids	Solenoporaceans	Tubiphytes	<i>Cuneolina</i> sp.	Micrite	Inoceramids	Planktonic foraminifers	Lagenids	Calcspheres and pithonellids	<i>Globigerinelloides ultramicrus</i>	<i>Globigerinelloides tentonensis</i>
29R-1, 109-114	379.89	—	—	—	—	—	—	—	—	—	—	—	—	—	—	—	—	VR AA	—	—	—	—	—	—	—
29R-2, 4-10	380.34	—	—	—	—	—	—	—	—	—	—	—	—	—	—	—	—	AA	—	—	—	—	—	—	—
30R-1, 15-20	388.55	—	—	—	—	—	—	R	—	—	—	—	—	—	—	—	—	? AAA	—	—	—	—	—	—	—
30R-1, 30-34	388.70	—	—	—	—	—	—	R/F	—	—	—	—	—	—	—	—	—	R/F A	—	—	—	—	—	—	—
30R-1, 55-59	388.95	—	—	—	—	—	—	F	—	—	—	—	—	—	—	—	—	F AAA	F	—	—	—	—	—	—
31R-1, 5-9	398.45	—	—	—	—	—	—	F/C	—	—	—	—	—	—	—	—	—	C/A	R AA R	—	—	—	—	—	—
32R-1, 12-14	407.82	—	—	—	—	R	AA	—	—	—	—	—	—	—	—	—	—	F	VR AAA R	—	—	—	—	—	—
32R-1, 56-60	408.26	C	—	—	—	—	—	—	—	—	—	—	—	—	—	—	—	F/C	R/F AAA	—	—	—	—	—	—
33R-1, 7-10	417.47	C	—	—	—	—	—	—	—	—	—	—	—	—	—	—	—	R	—	—	—	—	—	—	—
34R-1, 9-13	427.09	R F	—	R	R	—	—	R	—	—	—	—	—	—	—	—	—	VR AAA	VR	—	—	—	—	—	—
35R-1, 2-5	436.62	F F	VR	—	VR	R	AAA	—	VR	—	—	—	—	—	—	—	—	VR AAA	VR	—	—	—	—	—	—
35R-1, 13-15	436.73	AAA	—	—	—	—	—	—	—	—	—	—	—	—	—	—	—	AA	—	—	—	—	—	—	—
36R-1, 0-5	466.20	C A	F F	—	F/C R	—	C/A	—	F	—	VR VR	?	?	—	—	—	—	—	—	—	—	—	—	—	—
36R-1, 6-9	446.26	A	R	—	—	—	—	—	—	—	—	—	—	—	—	—	—	—	—	—	—	—	—	—	—
37R-1, 0-5	455.90	A	R	—	—	—	—	—	—	—	—	—	—	—	—	—	—	—	—	—	—	—	—	—	—
37R-1, 5-9	455.95	C	C	—	—	—	—	—	—	—	—	—	—	—	—	—	—	—	—	—	—	—	—	—	—
37R-1, 9-13	455.99	A	R	—	—	—	—	—	—	—	—	—	—	—	—	—	—	—	—	—	—	—	—	—	—
37R-1, 13-16	456.03	—	C	VR VR	—	F/C F	—	VR VR	—	—	VR	—	—	—	—	—	—	—	—	—	—	—	—	—	—
39R-1, 0-3	475.10	R	F VR	—	F F	—	R/F R	—	—	—	—	—	—	—	—	—	—	—	—	—	—	—	—	—	—
39R-1, 4-10	475.14	F/C	C F F	—	R/F R	—	R	?	—	—	—	—	—	—	—	—	—	A	—	—	—	—	—	—	—
39R-1, 10-14	475.20	F	C F F	—	C	—	R	—	—	—	—	—	—	—	—	—	—	A	—	—	—	—	—	—	—
41R-1, 0-5	494.40	C F	F	—	F/C	—	R VR	R	?	—	—	—	—	—	—	—	—	AA	—	—	—	—	—	—	—
41R-1, 12-16	494.52	F C	C	—	C	—	VR	—	R/F VR	—	—	—	—	—	—	—	—	—	—	—	—	—	—	—	—
41R-1, 106-108	495.46	F C	R R	—	F	—	R R	F/C	—	—	—	—	—	—	—	—	—	A	—	—	—	—	—	—	—
45R-1, 14-16	532.94	—	F R	VR	R/F R	1	—	—	—	—	—	—	—	—	—	—	—	F	—	—	—	—	—	—	—
45R-1, 18-20	532.98	VR	R VR	—	—	—	—	—	—	—	—	—	—	—	—	—	—	R	—	—	—	—	—	—	—
46R-1, 1-3	542.51	F	F R	VR	—	—	—	—	—	—	—	—	—	—	—	—	—	F	—	—	—	—	—	—	—
46R-1, 10-12	542.60	VR	R VR	—	—	—	—	—	—	—	—	—	—	—	—	—	—	F	—	—	—	—	—	—	—
49R-1, 8-12	571.48	—	—	—	—	—	—	—	—	—	—	—	—	—	—	—	AAA	—	—	—	—	—	—	—	—
49R-1, 13-17	571.53	F R	R R	?	—	—	—	—	—	—	—	—	—	—	—	—	AAA	—	—	—	—	—	—	—	—
50R-1, 0-4	581.00	F R/F	F VR	?	—	—	—	—	—	—	—	—	—	—	—	—	—	AAA	—	—	—	—	—	—	—
50R-1, 8-12	581.08	R	—	—	—	—	—	—	—	—	—	—	—	—	—	—	—	AAA	—	—	—	—	—	—	—

Note: Study conducted in thin sections. 1 = one fragment; X = present; VR = very rare (1-2 specimens); R = rare (2-5 specimens); C = common (10-30 specimens).

Table 2 (continued).

Planktonic foraminiferal assemblages exhibit a major change between Cores 160-967E-24R and 23R, with faunas in the latter core rich in globotruncanids along with common *Globotruncanita stuartiformis*, all of which are absent in Core 160-967E-24R. The assemblage in Sample 160-967E-23R-CC contains *V. eggeri* and *M. pseudolineiana* in association with *Globotruncana orientalis*. According to Caron (1985) and Nederbragt (1990) the co-occurrence of these species is indicative of the *G. elevata* Zone, although the zonal marker was never found in Hole 967E.

This zonal assignment is in agreement with the Campanian age inferred from calcareous nannofossils: Sample 160-967E-23R-CC yielded the nannofossil *Aspidiscus parcus*, which identifies the early Campanian CC18 Zone (Emeis, Robertson, Richter, et al., 1996) (Fig. 2). Owing to the poor recovery and size-sorting that affects all the assemblages, we attribute to the *G. elevata* Zone only Core 160-967E-23R.

Globotruncana ventricosa Zone (from 160-967E-22R-CC to 160-967E-20R-CC; 37.8 m).

Diagnosis: Interval from the FO of the zonal marker to the FO of *Radotruncana calcarata*.

The zonal marker *Globotruncana ventricosa* was identified with certainty only much higher in the following zone. In the absence of the zonal marker, zonal attribution was based on the appearance of *Globotruncana rosetta* in Sample 160-967E-22R-1, 19–22 cm, in association with *Globotruncana arca*, *G. orientalis*, *G. linneiana*, and *G. mariei*. Above this level, several species first appear in succession, such as *Pseudotextularia elegans* and *Globigerinelloides alvarezi* in Sample 160-967E-21R-CC, and *Contusotruncana plummerae* and *C. patelliformis* in Sample 160-967E-21R-1, 46–48 cm. According to Robaszynski et al. (1984), Caron (1985), and Premoli Silva and Sliter (1994) the successive appearances of the aforementioned species are recorded within the *G. ventricosa* Zone.

Radotruncana calcarata Zone (from 160-967E-19R-CC to 160-967E-19R-1, 69–71 cm; 1.1 m)

Diagnosis: Total range of the zonal marker.

Rare specimens of the named taxon were identified in both samples from Core 160-967E-19R. The assemblages are very similar to those from the previous zone. In addition to the species inherited from the *G. ventricosa* Zone, common *G. ventricosa* and abundant *Pseudoguembelina costulata* were also found.

Globotruncanella havanensis Zone (from 160-967E-18R-3, 51–53 cm, to 160-967E-17R-2, 127–134 cm; 18.62 m)

Diagnosis: Interval from the LO of *Radotruncana calcarata* to the FO of *Globotruncana aegyptiaca*.

This zone was identified according to its definition, although in the absence of the zonal marker. Several additional species are recorded at the base of this zone, such as *Globotruncanita stuarti*, *Globotruncana falsostuarti*, *Globotruncanella minuta*, and the rugoglobigerinids, followed above by the appearance of *Ventilabrella multicamerata*, *Heterohelix punctulata*, and *Rugoglobigerina rugosa*. *Heterohelix carinata* is last recorded at the base of the zone.

Globotruncana aegyptiaca Zone (from 160-967E-17R-1, 117–120 cm, to 160-967E-15R-3, 30–34 cm; 17.72 m)

Diagnosis: Interval from the FO of the zonal marker to the FO of *Gansserina gansseri*.

The zonal marker is rare. Several additional species were found in this zone such as *Laeviheterohelix dentata*, *Pseudoguembelina palpebra*, *Rugoglobigerina macrocephala*, and *Globotruncanella havanensis* at the base, followed by *Heterohelix planata*, *Globotrunc-*

canella pschadai, and *Heterohelix labellosa*, *Rugoglobigerina hexacamerata*, and *R. pennyi* in the upper part of the zone.

The overall preservation of planktonic faunas improves in this interval and size-sorting is less marked.

Gansserina gansseri Zone (from 160-967E-15R-2, 122–124 cm, to 160-967E-10R-3, 60–62 cm; 48.05 m)

Diagnosis: Interval from the FO of the zonal marker to the FO of *Contusotruncana contusa*.

The zonal marker is very rare and scattered throughout the zone. *Abathomphalus intermedius* and *Planoglobulina carseyae* appear at the base of the zone, followed by the FO of *Globotruncanita pettersi*, *Kuglerina rotundata*, *Pseudoguembelina excolata*, *Gansserina wiedermayeri*, *Globotruncana esnehensis*, *Globotruncanita conica*, *Gublerina acuta*, *Pseudotextularia nuttalli*, and *Gublerina cuvilli*. Close to the top of the zone, *Planoglobulina acervulinoidea*, *Pseudotextularia intermedia*, and *Plummerita hantkeninoides* are also recorded. *Globigerinelloides bollii* disappears in the middle part of the zone followed slightly higher by the disappearance of *G. prairiehillensis*.

Contusotruncana contusa/Racemiguembelina fructicosa Zone (from 160-967E-10R-3, 0–4 cm, to 160-967E-10R-2, 0–3 cm; 1.56 m)

Diagnosis: Interval from the FO of the zonal markers to the FO of *Abathomphalus mayaroensis*.

The lower boundary of this short zone was identified by the presence of the first of the two markers only, whereas the second marker appears just prior to the end of the zone. *Contusotruncana plummerae* and *Heterohelix rajagopalani* disappear at the end of the zone.

Abathomphalus mayaroensis Zone (from 160-967E-10R-1, 114–117 cm, to 160-967E-8R-2, 50–52 cm; 19.04 m)

Diagnosis: Interval from the FO of the zonal marker to the extinction of most of the Cretaceous planktonic foraminifers, almost equated to the total range of the zonal marker.

The zonal marker is rather common throughout the zone. Preservation becomes increasingly poor toward the top, and in the uppermost sample the assemblage is composed mainly of small-sized heterohelicids or fragmented *P. elegans*. The rotaliiforms are practically absent above Sample 160-967E-8R-CC.

The first sample belonging to the Tertiary is Sample 160-967E-8R-1, 92–94 cm, which contains a strongly mixed assemblage that spans the interval from the earliest Paleocene Zone Palpa to the late early Oligocene.

Oligocene Planktonic Foraminifers

Oligocene planktonic foraminiferal assemblages are scarce and poorly preserved throughout (Sample 160-967E-8R-1, 92–94 cm, to 3R-1, 57–59 cm) (Fig. 3). The sedimentary sequence cannot be attributed to an interval older than the early Oligocene, possibly Zone P20, based on the presence of *Cassigerinella chipolensis* and *Paragloborotalia siakensis* in several samples. Oligocene specimens are, however, very rare and overwhelmed by reworked specimens.

Reworking includes the typical middle Eocene planktonic species previously observed in Hole 966F, together with common early to mid-Paleocene and early Eocene forms such as, *Parvularugoglobigerina eugubina*, *Globanomalina planocompressa*, *Globoconus daubjergensis*, *Praemurica uncinata*, *Praemurica praecursoria*, *Subbotina triloculinoides*, *Parasubbotina pseudobulloides*, *Acarinina mckennai*, *Morozovella angulata* (Paleocene Zones Palpa to P3b); *Acarinina nitida*, *Morozovella quetra*, *M. gracilis*, *M. subbotinae*, *M. occlusa* (early Eocene Zones P6b to P7); and *Acarinina cuneicamerata* and *A. spinuloinflata* (middle Eocene Zones P10–P11).

There is no evidence of planktonic foraminiferal assemblages attributable to the late Paleocene, late early Eocene, latest Eocene, and probably earliest Oligocene. Because of the strong reworking, no range chart was produced for this hole.

Cretaceous Sedimentation Rate

To identify the presence of possible hiatuses, owing to the non-documentation of some zones and the overall poor recovery, a mean sedimentation rate of 8.17 m/m.y. was estimated for the entire sequence from the *H. helvetica* Zone to the *A. mayaroensis* Zone (178.0–407.7 mbsf; total thickness, 229.7 m) (Fig. 4), based on the time scale of Erba et al. (1995). As shown in Figure 4 (see also Table 4), the sedimentation rate varies from zone to zone. In particular, very low rates are apparent in the *G. elevata* (2.38 m/m.y.), *R. calcarata* (2.02 m/m.y.), and *C. contusa* (1.04 m/m.y.) Zones. It is worth mentioning that the zonal markers of these three zones are usually large-sized forms (>250 µm). As described above, most of the larger fractions of the residues were removed by either winnowing or resedimentation favoring the accumulation of smaller species and specimens. Consequently, what we observed was probably not the true range of the marker species, resulting in an underestimation of the thickness of the single zones and an artificially low sedimentation rate. Recalculating the sedimentation rates for the intervals from the base of the *G. gansseri* Zone to the top of the *A. mayaroensis* Zone, and from the base of the *G. elevata* Zone to the base of the *G. gansseri* Zone, we obtained sedimentation rates close to the mean value (8.73 m/m.y. and 8.08 m/m.y., respectively). This recalculation supports the continuity of sedimentation during the Campanian-Maastrichtian (Fig. 4).

In the sequence below the *G. elevata* Zone, the *D. asymmetrica* Zone displaces a sedimentation rate slightly higher than the mean value (9.32 m/m.y.), whereas a sedimentation rate higher than 11.0 m/m.y. was estimated for the *D. concavata* Zone, the best documented zone.

The *D. concavata* Zone directly overlies the lower part of the *H. helvetica* Zone. As described above, the *M. sigali* Zone and the middle to upper part of the *H. helvetica* Zone were not identified. The calculation of the sedimentation rate assuming that the *H. helvetica* Zone is totally represented resulted in a value much lower than the mean rate (3.87 m/m.y.). Recalculating the sedimentation rate for the interval from the top of the *D. concavata* Zone to the supposed base of the *H. helvetica* Zone, we obtained a sedimentation rate of 5.97 m/m.y., a value still lower than the mean rate. This suggests that the *M. sigali* Zone and the middle to upper part of the *H. helvetica* Zone may indeed be missing.

Cretaceous Isotope Stratigraphy

Oxygen and carbon isotopes were measured in bulk samples in order to tentatively compare the Hole 967E record with the isotope curves previously obtained in continuous and well-dated land sections (Corfield et al., 1991; Jenkyns et al., 1994). As shown in Figure 5, the stratigraphic resolution is rather poor, especially in the lower part of the sedimentary sequence below the *R. calcarata* Zone, owing to very poor recovery.

The oxygen and carbon curves frequently display opposite trends (see also Table 5). This may suggest that diagenesis altered little of the primary signals (Corfield et al., 1991). The oxygen curve shows a trend toward more positive values from the bottom to the top of the pelagic sequence, and the carbon curve shows more constant values with low amplitude fluctuations throughout, a pattern similar to that observed by Corfield et al. (1991) in the Bottaccione section (Gubbio, Italy). Two negative carbon peaks in the *D. concavata* Zone may correspond to the negative peaks shown by Jenkyns et al. (1994), with the lower one equated to the base of the Coniacian. This lower shift is used to place the base of the Coniacian as shown in Figure 4. The

other two negative carbon peaks, at the base of the *G. havanensis* Zone (late Campanian) and in the lower part of the *G. gansseri* Zone (early Maastrichtian), may correlate with those identified by Corfield et al. (1991) as reinterpreted according to Premoli Silva and Sliter (1994). The prominent negative carbon shift related to the Bonarelli Event (latest Cenomanian) (Corfield et al., 1991; Jenkyns et al., 1994) was not recorded in Hole 967E.

Shallow-water sediments and sediments transitional between shallow-water carbonates and pelagic chalk display more negative oxygen and carbon isotope values. The more negative carbon isotope value is consistent with the late Aptian age attributed to the upper part of the carbonate platform and seems to correspond to the negative shift observed close to the Aptian/Albian boundary in the Italian pelagic sequences as reported in Erba (1996).

SUMMARY AND CONCLUSIONS

Despite the poor recovery, poor preservation of planktonic foraminifers, intense winnowing, and some reworking, Leg 160 recovered a relatively continuous Upper Cretaceous pelagic succession from the lower slope of the Eratosthenes Seamount. Only the *M. sigali* Zone and the middle to late *H. helvetica* Zone of middle Turonian age were not documented. The very low rate of sedimentation estimated from the top of the *D. concavata* Zone (early Santonian) to the base of the *H. helvetica* Zone (early Turonian) suggests that the *M. sigali* Zone and the middle to late *H. helvetica* Zone are probably missing.

Below the lower *H. helvetica* Zone, biostratigraphic resolution is very poor owing to sparse planktonic foraminifers and the apparent absence of calcareous nannofossils. However, the initiation of pelagic sedimentation on the seamount can probably be dated to the mid-Cenomanian. The top of the shallow-water carbonate unit is well dated to the late Aptian based on the presence of *Archaealveolina reicheli*. The same age-diagnostic larger foraminifer is reworked within the lowermost pelagic layers. There is no evidence that sediments of Albian to early Cenomanian age were ever deposited. This suggests that shallow-water deposition ended in the late Aptian, and a hiatus probably spans the entire Albian and part of the Cenomanian. The lower part of the shallow-water sequence cannot be dated.

Another major hiatus marks the Cretaceous/Tertiary boundary, with early Oligocene sediments resting on those of the late Maastrichtian. However, from the reworked assemblages we can infer that deposition on the seamount was much more complete: in fact, the lower to mid-Paleocene, and parts of the lower and middle Eocene could be documented. The missing upper Paleocene, part of the lower Eocene, and upper Eocene were either not deposited or were removed to lower levels in the basin and bypassed the Site 967 location. The heavy reworking may indicate tectonic instability or a higher energy environment during the early Oligocene.

Pelagic sedimentation occurred atop the seamount in the middle Eocene as indicated by the rather undisturbed pelagic record recovered in Hole 966F. At this topographically higher location, however, pelagic sedimentation was much less continuous than in the lower slope, suggesting that the Site 966 location was possibly the source area of the downslope reworked material.

Stable isotope stratigraphy (oxygen and carbon) tentatively allows comparison of the Cretaceous isotope record of Hole 967E with continuous and well-dated land sections in central Italy. One of the negative carbon isotope peaks was recognized as indicative of the base of the Coniacian.

ACKNOWLEDGMENTS

The second author is indebted to ODP for inviting her to participate in Leg 160. The authors would like to thank Maurizio Chiocchini

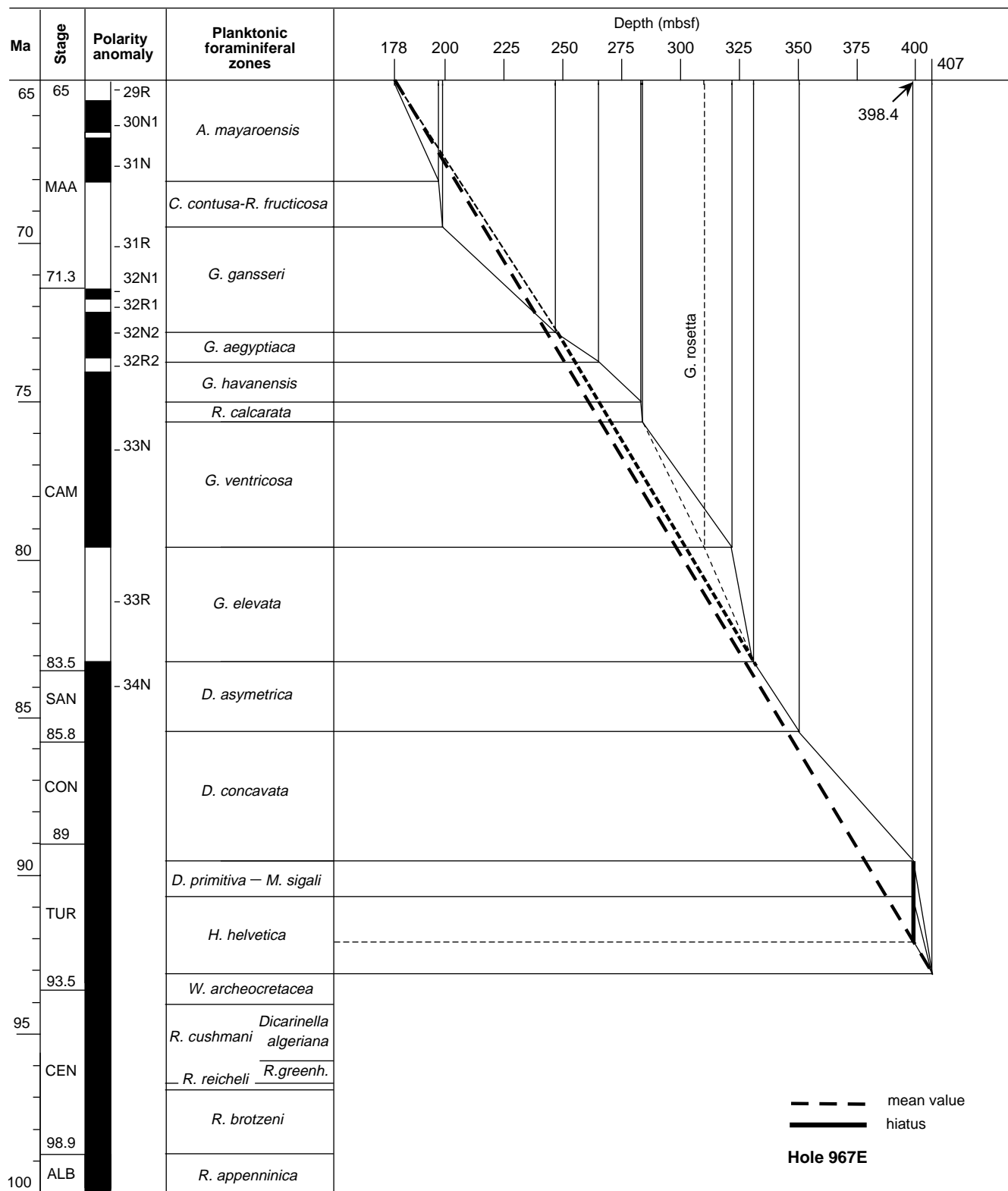


Figure 4. Sedimentation rate of the Cretaceous succession recovered from Hole 967E plotted vs. planktonic foraminiferal zonal scheme, magnetic polarity, and time scale from Erba et al. (1995). See text section "Cretaceous Sedimentation Rate," for explanation.

Table 4. Cretaceous planktonic foraminiferal zones vs. their thickness and sedimentation rate, Hole 967E.

Cretaceous planktonic foraminiferal zones	Thickness (m)	Sedimentation rate (m/m.y.)
<i>A. mayaroensis</i>	19.00	6.33
<i>C. contusa</i>	1.56	1.04
<i>G. gansseri</i>	48.05	13.73
<i>G. aegyptiaca</i>	17.72	17.72
<i>G. havanensis</i>	18.72	12.48
<i>R. calcarata</i>	1.01	2.02
<i>G. ventricosa</i>	37.80	9.45
<i>G. elevata</i>	8.82	2.38
<i>D. asymmetrica</i>	19.58	9.32
<i>D. concavata</i>	>45.0	>11.0
<i>H. helvetica</i>	9.30	3.87

Notes: Time scale after Erba et al. (1995). The thickness of *D. concavata* Zone is poorly constrained because of the very poor recovery.

for his help and suggestions concerning the interpretation of shallow-water facies. W.V. Sliter and B. Huber are greatly acknowledged for reviewing the paper. This research was partially supported by the Italian Consiglio Nazionale delle Ricerche CT Grant no. 94.00168.CT05 to M.B. Cita.

REFERENCES

- Arnaud Vanneau, A., and Premoli Silva, I., 1995. Biostratigraphy and systematic description of benthic foraminifers from mid-Cretaceous shallow-water carbonate platform sediments at Sites 878 and 879 (MIT and Takuyo-Daisan Guyots). In Haggerty, J.A., Premoli Silva, I., Rack, F., and McNutt, M.K. (Eds.), *Proc. ODP, Sci. Results*, 144: College Station, TX (Ocean Drilling Program), 199–219.
- Blow, W.H., 1969. Late middle Eocene to Recent planktonic foraminiferal biostratigraphy. In Brönnimann, P., and Renz, H.H. (Eds.), *Proc. First Int. Conf. Planktonic Microfossils*, Geneva, 1967: Leiden (E.J. Brill), 1:199–422.
- , 1979. *The Cainozoic Globigerinida*: Leiden (E.J. Brill).
- Boersma, A., and Premoli-Silva, I., 1983. Paleocene planktonic foraminiferal biogeography and the paleoceanography of the Atlantic Ocean. *Micropaleontology*, 29:355–381.
- Boersma, A., Premoli Silva, I., and Shackleton, N.J., 1987. Atlantic Eocene planktonic foraminiferal paleohydrographic indicators and stable isotope paleoceanography. *Paleoceanography*, 2:287–331.
- Caron, M., 1985. Cretaceous planktic foraminifera. In Bolli, H.M., Saunders, J.B., and Perch-Nielsen, K. (Eds.), *Plankton Stratigraphy*: Cambridge (Cambridge Univ. Press), 17–86.
- Corfield, R.M., Cartlidge, J.E., Premoli Silva, I., and Housley, R.A., 1991. Oxygen and carbon isotope stratigraphy of the Palaeogene and Cretaceous limestones in the Bottaccione Gorge and the Contessa Highway sections, Umbria, Italy. *Terra Nova*, 3:414–422.
- Craig, H., 1957. Isotopic standards for carbon and oxygen and correction factors for mass-spectrometric analysis of carbon dioxide. *Geochim. Cosmochim. Acta*, 12:133–149.
- De Castro, P., 1966. Contributo alla conoscenza delle Alveoline albiano-cenomaniane della Campania. *Boll. Soc. Natural. Napoli*, 75:1–59.
- Emeis, K.-C., Robertson, A.H.F., Richter, C., et al., 1996. *Proc. ODP, Init. Repts.*, 160: College Station, TX (Ocean Drilling Program).
- Erba, E., 1996. The Aptian Stage. In Rawson, P.F., Dhondt, A.V., Hancock, J.M., and Kennedy, W.J. (Eds.), *Proc. 2nd Int. Symp. on Cretaceous Stage Boundaries*, 8–16 Sept. 1995. *Bull. Inst. R. Sci. Nat. Belg.*, 66 (Suppl.):31–43.
- Erba, E., Premoli Silva, I., Wilson, P.A., Pringle, M.S., Sliter, W.V., Watkins, D.K., Arnaud Vanneau, A., Bralower, T.J., Budd, A.F., Camoin, G.F., Masse, J.-P., Mutterlose, J., and Sager, W.W., 1995. Synthesis of stratigraphies from shallow-water sequences at Sites 871 through 879 in the western Pacific Ocean. In Haggerty, J.A., Premoli Silva, I., Rack, F., and McNutt, M.K. (Eds.), *Proc. ODP, Sci. Results*, 144: College Station, TX (Ocean Drilling Program), 873–885.
- Fourcade, E., 1980. *Archaealveolina decastroi* n. gen. n. sp. Foraminifère nouveau de l' Aptien supérieur de l'Ile d'Ibiza (Espagne). *Rev. Micropaleontol.*, 23:67–75.
- Hemleben, C., Muhlen, D., Olsson, R.K., and Berggren, W.A., 1991. Surface texture and the first occurrence of spines in planktonic foraminifera from the early Tertiary. *Geol. Jahrb.*, 128:117–146.
- Jenkins, H.C., Gale, A.S., and Corfield, R.M., 1994. Carbon- and oxygen-isotope stratigraphy of the English Chalk and Italian Scaglia and its palaeoclimatic significance. *Geol. Mag.*, 131:1–34.
- Loeblich, A.R., Jr., and Tappan, H., 1988. *Foraminiferal Genera and Their Classification*: New York (Van Nostrand Reinhold).
- Nederbragt, A.J., 1990. Biostratigraphy and paleoceanographic potential of the Cretaceous planktic foraminifera Heterohelicidae. [Doctoral diss.]. Centrale Huisdrukkerij Vrije Univ., Amsterdam.
- Olsson, R.K., Hemleben, C., Berggren, W.A., and Liu, C., 1992. Wall texture classification of planktonic Foraminifera Genera in the lower Danian. *J. Foraminiferal Res.*, 22:195–213.
- Pessagno, E.A., 1967. Upper Cretaceous planktonic foraminifera from the western Gulf Coastal Plain. *Paleontograph. Am.*, 5:245–445.
- Premoli Silva, I., and Boersma, A., 1988. Atlantic Eocene planktonic foraminiferal historical biogeography and paleohydrographic indices. *Palaeogeogr., Palaeoclimatol., Palaeoecol.*, 67:315–356.
- , 1989. Atlantic Paleogene planktonic foraminiferal bioprovincial indices. *Mar. Micropaleontol.*, 14:357–371.
- Premoli Silva, I., and Sliter, W.V., 1994. Cretaceous planktonic foraminiferal biostratigraphy and evolutionary trends from the Bottaccione Section, Gubbio, Italy. *Palaeontogr. Ital.*, 82:2–90.
- Robaszynski, F., and Caron, M., 1995. Foraminifères planctoniques du Crétacé: commentaire de la zonation Europe-Méditerranée. *Bull. Soc. Geol. Fr.*, 166:681–692.
- Robaszynski, F., Caron, M., Dupuis, C., Amedro, F., Gonzales-Donoso, J.M., Linares-Rodriguez, D., Hardenbol, J., Gartner, S., Calandra, F., and Deloffre, R., 1990. A tentative integrated stratigraphy in the Turonian of Central Tunisia: formations, zones and sequential stratigraphy in the Kalaat Senan area. *Bull. Cent. Res. Expl.—Prod. ELF-Aquitaine*, 14:213–384.
- Robaszynski, F., Caron, M. (Coord.), and the European Working Group on Planktonic Foraminifera, 1979. *Atlas de Foraminifères Planctoniques du Crétacé Moyen (Vols. 1 and 2)*. Cah. Micropaleontol.
- Robaszynski, F., Caron, M., Gonzales-Donoso, J.-M., Wonders, A.A.H., and the European Working Group on Planktonic Foraminifera, 1984. Atlas of Late Cretaceous globotruncanids. *Rev. Micropaleontol.*, 26:145–305.
- Robaszynski, F., Hardenbol, J., Caron, M., Amédro, F., Dupuis, C., González Donoso, J.-M., Linares, D., and Gartner, S., 1993. Sequence stratigraphy in a distal environment: the Cenomanian of the Kalaat Senan region (central Tunisia). *Bull. Cent. Rech. Expl.—Prod. Elf-Aquitaine*, 17:395–433.
- Spezzaferri, S., 1994. Planktonic foraminiferal biostratigraphy and taxonomy of the Oligocene and lower Miocene in the oceanic record: an overview. *Palaeontographia Ital.*, 81:1–187.
- Toumarkine, M., and Luterbacher, H., 1985. Paleocene and Eocene planktic foraminifera. In Bolli, H.M., Saunders, J.B., and Perch-Nielsen, K. (Eds.), *Plankton Stratigraphy*: Cambridge (Cambridge Univ. Press), 87–154.

Date of initial receipt: 7 January 1997

Date of acceptance: 10 August 1997

Ms 160SR-022

LIST OF SPECIES

Species are listed in alphabetical order by genus.

List of Paleogene Species

The generic and specific concepts and the species groups used by Boersma and Premoli Silva (1983), Boersma et al. (1987), Olsson et al. (1992), Premoli Silva and Boersma (1988, 1989), and Spezzaferri (1994) are retained herein, whenever possible.

Acarinina bullbrooki (Bolli, 1957) (= *Globorotalia bullbrooki* Bolli)

Acarinina matthewsae (Blow, 1979) (= *Globorotalia (Acarinina) matthewsae* Blow)

Acarinina pentacamerata Subbotina, 1953

Acarinina primitiva (Finlay, 1939) (= *Globoquadrina primitiva* Finlay)

Acarinina pseudotopilensis Subbotina, 1953

Acarinina rugosoculaeata Subbotina, 1953

Cassigerinella chipolensis (Cushman and Ponton, 1932) (= *Cassidulina chipolensis* Cushman and Ponton)

Catapsydrax unicavus Bolli, Loeblich and Tappan, 1957

Chilogumbelina cubensis (Palmer, 1934) (= *Guembelina cubensis* Palmer).

- Dentoglobigerina galavisi* (Bermudez, 1961) (= *Globigerina galavisi* Bermudez)
"Globigerina" venezuelana Hedberg, 1937
Globigerinatheka index (Finlay, 1939) (= *Globigerinoides index* Finlay)
Globigerinatheka luterbacheri Bolli, 1972
Globigerinatheka micra (Shutskaya, 1958) (= *Globigerinoides subconglobatus* var. *micra* Shutskaya)
Globigerinatheka subconglobata (Shutskaya, 1958) (= *Globigerinoides subconglobatus* Chalilov var. *subconglobata* Chalilov).
Globorotaloides carcosellensis Toumarkine and Bolli, 1975
Morozovella aragonensis (Nuttall, 1930) (= *Globorotalia aragonensis* Nuttall)
Igorina broedermannii (Cushman and Bermudez) (= *Globorotalia (Truncorotalia) broedermannii* Cushman and Bermudez)
Morozovella lenheri (Cushman and Jarvis, 1929) (= *Globorotalia lenheri* Cushman and Jarvis)
Paragloborotalia siakensis (LeRoy, 1939) (= *Globorotalia siakensis* LeRoy)
Globanomalina pseudoscitulus (Glaessner, 1937) (= *Globorotalia pseudo-scutula* Glaessner)
Pseudohastigerina micra (Cole, 1927) (= *Nonion micrus* Cole)
Subbotina angiporoidea angiporoidea (Hornbrook, 1965) (= *Globigerina angiporoidea* Hornbrook)
Subbotina angiporoidea minima (Jenkins, 1966) (= *Globigerina angiporoidea* Hornbrook subsp. *minima* Jenkins)
Subbotina eocaena (Guembel, 1868) (= *Globigerina eocaena* Guembel).
Subbotina hornibrooki (Brönnimann, 1952) (= *Globigerina hornibrooki*, Brönnimann)
Subbotina inaequispira (Subbotina, 1953) (= *Globigerina inaequispira* Subbotina)
Subbotina linaperta (Finlay, 1939) (= *Globigerina linaperta* Finlay).
Subbotina praeturritilina (Blow and Banner, 1962) (= *Globigerina turritilina praeturritilina* Blow and Banner).
Subbotina utilisindex (Jenkins and Orr, 1973) (= *Globigerina utilisindex* Jenkins and Orr)
Tenuitella gemma (Jenkins, 1971) (= *Globorotalia (Turborotalia) gemma* Jenkins)
Truncorotaloides rohri Brönnimann and Bermudez, 1953
Truncorotaloides topilensis (Cushman, 1925) (= *Globigerina topilensis* Cushman)
Turborotalia boweri (Bolli, 1957) (= *Globorotalia boweri* Bolli)
Turborotalia cerroazulensis (Cole, 1928) (= *Globigerina cerro-azulensis* Cole)
Turborotalia griffinae Blow, 1979
Turborotalia pomeroli (Toumarkine and Bolli, 1970) (= *Globorotalia cerroazulensis pomeroli* Toumarkine and Bolli)
Turborotalia praecentralis Blow, 1979
Turborotalia pseudoampliatura (Blow and Banner, 1962) (= *Globigerina pseudoampliatura* Blow and Banner).
Turborotalia pseudomayeri (Bolli, 1959) (= *Globigerina pseudomayeri* Bolli)
Zeaglobigerina ampliatura (Bolli, 1957) (= *Globigerina ampliatura* Bolli)
- List of Cretaceous Species**
- The generic and specific concepts follow Pessagno (1967), Robaszynski et al. (1979, 1984, 1990), Caron (1985), Loeblich and Tappan (1988), Nederbragt (1990), and Premoli Silva and Sliter (1994).
- Abathomphalus intermedius* (Bolli, 1951) (= *Globotruncana intermedia* Bolli)
Abathomphalus mayaroensis (Bolli, 1951) (= *Globotruncana mayaroensis* Bolli)
Archaeoglobigerina blowi Pessagno, 1967
Archaeoglobigerina cretacea (d' Orbigny, 1840) (= *Globigerina cretacea* d' Orbigny)
Biglobigerinella multispira Lalicker, 1948
Clavihedbergella simplex (Morrow, 1934) (= *Hastigerinella simplex* Morrow)
Contusotruncana contusa (Cushman, 1926) (= *Pulvinulina arca* var. *contusa* Cushman)
Contusotruncana fornicate (Plummer, 1921) (= *Globotruncana fornicate* Plummer)
Contusotruncana patelliformis (Gandolfi, 1955) (= *Globotruncana patelliformis* Gandolfi)
Contusotruncana plicata (White, 1928) (= *Globotruncana conica* var. *plicata* White)
Contusotruncana plummerae (Gandolfi, 1955) (= *Globotruncana plummerae* Gandolfi)
Dicarinella asymmetrica (Sigal, 1952) (= *Globotruncana asymmetrica* Sigal)
Dicarinella canaliculata (Reuss, 1854) (= *Rosalina canaliculata* Reuss)
- Dicarinella concavata* (Brotzen, 1934) (= *Rotalia concavata* Brotzen)
Dicarinella hagni (Scheibnerova, 1962) (= *Praeglobotruncana hagni* Scheibnerova)
Dicarinella imbricata (Mornod, 1949) (= *Globotruncana imbricata* Mornod)
Dicarinella primitiva (Dalbiez, 1955) (= *Globotruncana ventricosa* subsp. *primitiva* Dalbiez)
Falsotruncana maslakvae Caron, 1981
Favusella washitensis (Carsey, 1926) (= *Globigerina washitensis* Carsey)
Gansserina gansseri (Bolli, 1951) (*Globotruncana gansseri* Bolli)
Gansserina wiedenmayeri (Gandolfi, 1955) (= *Globotruncana wiedenmayeri* Gandolfi)
Globigerinelloides alvarezi (Eternod Olvera, 1959) (= *Planomalina alvarezi* Eternod Olvera)
Globigerinelloides asper (Ehrenberg, 1854) (= *Phanerostomum asperum* Ehrenberg)
Globigerinelloides bentonensis (Morrow, 1934) (= *Anomalina bentonensis* Morrow)
Globigerinelloides bollii Pessagno, 1967
Globigerinelloides caseyi (Bolli, Loeblich and Tappan, 1957) (= *Planomalina caseyi* Bolli, Loeblich and Tappan)
Globigerinelloides messinae (Brönnimann, 1952) (= *Globigerinella messinae* Brönnimann)
Globigerinelloides prairiehillensis Pessagno, 1967
Globigerinelloides subcarinatus (Brönnimann, 1952) (= *Globigerinella messinae subcarinata* Brönnimann)
Globigerinelloides ultramicrus (Subbotina, 1949) (= *Globigerinella ultramicros* Subbotina)
Globotruncana aegyptiaca Nakkady, 1950
Globotruncana arca (Cushman, 1926) (= *Pulvinulina arca* Cushman)
Globotruncana bulloides Vogler, 1941
Globotruncana dupeuplei Caron, Gonzales Donoso, Robaszynski and Wonders, 1984
Globotruncana esnehensis Nakkady, 1950
Globotruncana falsostuarti Sigal, 1952
Globotruncana insignis Gandolfi, 1955
Globotruncana lapparenti Brotzen, 1936
Globotruncana linneiana (d' Orbigny, 1839) (= *Rosalina linneiana* d' Orbigny)
Globotruncana marie Banner and Blow, 1960
Globotruncana orientalis El Naggar, 1966
Globotruncana rosetta (Carsey, 1926) (= *Globigerina rosetta* Carsey)
Globotruncana rugosa (Marie, 1941) (= *Rosalinella rugosa* Marie)
Globotruncana ventricosa White, 1928
Globotruncanella havanensis (Voorwijk, 1937) (= *Globotruncana havanensis* Voorwijk)
Globotruncanella minuta Caron and Gonzales Donoso, 1984
Globotruncanella petaloidea (Gandolfi, 1955) (= *Globotruncana (Rugoglobigerina) petaloidea* Gandolfi)
Globotruncanella pschadai (Keller, 1946) (= *Globorotalia pschadai* Keller)
Globotruncanita angulata (Tilev, 1951) (= *Globotruncana lugeoni* var. *angulata* Tilev)
Globotruncanita conica (White, 1928) (= *Globotruncana conica* White)
Globotruncanita pettersi (Gandolfi, 1955) (= *Globotruncana rosetta* Pettersi Gandolfi)
Globotruncanita stuarti (de Lapparent, 1918) (= *Rosalina stuarti* de Lapparent)
Globotruncanita stuartiformis (Dalbiez, 1955) (= *Globotruncana stuartiformis* Dalbiez)
Gublerina acuta de Klasz, 1953
Gublerina cuvilliieri Kikoine, 1948
Guembelitria cretacea Cushman, 1933
Hedbergella delrioensis (Carsey, 1926) (= *Globigerina cretacea* var. *delrioensis* Carsey)
Hedbergella flandriini Porthault, 1970
Hedbergella holmdelensis Olsson, 1964
Hedbergella monmouthensis (Olsson, 1960) (= *Globorotalia monmouthensis* Olsson)
Hedbergella planispira (Tappan, 1940) (= *Globigerina planispira* Tappan)
Helvetoglobotruncana helvetica (Bolli, 1945) (= *Globotruncana helvetica* Bolli)
Heterohelix carinata (Cushman, 1938) (= *Guembelina carinata* Cushman)
Heterohelix globulosa (Ehrenberg, 1840) (= *Textularia globulosa* Ehrenberg)
Hetrohelix labellosa Nederbragt, 1990
Heterohelix moremani (Cushman, 1938) (= *Guembelina moremani* Cushman)
Heterohelix navarroensis Loeblich, 1951
Heterohelix punctulata (Cushman, 1938) (= *Guembelina punctulata* Cushman)

- Heterohelix planata* (Cushman, 1938) (= *Guembelina planata* Cushman)
Heterohelix rajagopalani (Govindan, 1972) (= *Gublerina rajagopalani* Govindan)
Heterohelix reussi (Cushman, 1938) (= *Guembelina reussi* Cushman)
Heterohelix sphenoides Masters, 1976
Heterohelix striata (Ehrenberg, 1840) (= *Textularia striata* Ehrenberg)
Kefiana sp.
Kuglerina rotundata (Brönnimann, 1952) (= *Rugoglobigerina rugosa rotunda* Brönnimann)
Laeviheterohelix dentata Stenestad, 1968
Laeviheterohelix pulchra (Brotzen, 1936) (= *Guembelina pulchra* Brotzen)
Laeviheterohelix turgida Nederbragt, 1990
Marginotruncana coronata (Bolli, 1945) (= *Globotruncana lapparenti* subsp. *coronata* Bolli)
Marginotruncana marginata (Reuss, 1845) (= *Rosalina marginata* Reuss)
Marginotruncana pseudolinneiana Pessagno, 1967
Marginotruncana renzi (Gandolfi, 1942) (= *Globotruncana renzi* Gandolfi)
Marginotruncana schneegansi (Sigal, 1952) (= *Globotruncana schneegansi* Sigal)
Marginotruncana sigali (Reichel, 1950) (= *Globotruncana sigali* Reichel)
Marginotruncana sinuosa Porthault, 1970
Planoglobulina acervulinoides (Egger, 1899) (= *Guembelina acervulinoides* Egger)
Planoglobulina carseyae (Plummer, 1931) (= *Ventilabrella carseyae* Plummer)
Planoglobulina riograndensis (Martin, 1972) (= *Ventilabrella riograndensis* Martin)
Plummerita hantkeninoides (Brönnimann, 1952) (= *Rugoglobigerina hantkeninoides* Brönnimann)
Praeglobotruncana gibba Klaus, 1960
Praeglobotruncana stephani (Gandolfi, 1942) (= *Globotruncana stephani* Gandolfi)
Pseudoguembelina costellifera Masters, 1976
- Pseudoguembelina costulata* (Cushman, 1938) (= *Guembelina costulata* Cushman)
Pseudoguembelina excolata (Cushman, 1926) (= *Guembelina excolata* Cushman)
Pseudoguembelina hariaensis Nederbragt, 1990
Pseudoguembelina kempensis Esker, 1968
Pseudoguembelina palpebra Brönnimann and Brown, 1953
Pseudotextularia elegans (Rzehak, 1891) (= *Cuneolina elegans* Rzehak)
Pseudotextularia intermedia de Klasz, 1953
Pseudotextularia nuttalli (Voorwijk, 1937) (= *Guembelina nuttalli* Voorwijk)
Racemiguembelina fructicosa (Egger, 1899) (= *Guembelina fructicosa* Egger)
Radotruncana calcarata (Cushman, 1927) (= *Globotruncana calcarata* Cushman)
Rugoglobigerina hexacamerata Brönnimann, 1952
Rugoglobigerina macrocephala Brönnimann, 1952
Rugoglobigerina milamensis Smith and Pessagno, 1973
Rugoglobigerina pennyi Brönnimann, 1952
Rugoglobigerina reicheli Brönnimann, 1952
Rugoglobigerina rugosa (Plummer, 1926) (= *Globigerina rugosa* Plummer)
Rugotruncana sp.
Sigalia decoratissima carpatica Salaj and Samuel, 1963
Sigalia deflaensis rugocostata Nederbragt, 1990
Ventilabrella eggeri Cushman, 1928
Ventilabrella multicamerata (de Klasz, 1953) (= *Planoglobulina multicamerata* de Klasz)
Whiteinella aprica (Loeblich and Tappan, 1961) (= *Hedbergella aprica* Loeblich and Tappan)
Whiteinella archaeocretacea Pessagno, 1967
Whiteinella baltica Douglas and Rankin, 1969
Whiteinella paradubia (Sigal, 1952) (= *Globigerina paradubia* Sigal)
Whiteinella praehelvetica (Trujillo, 1960) (= *Rugoglobigerina praehelvetica* Trujillo)

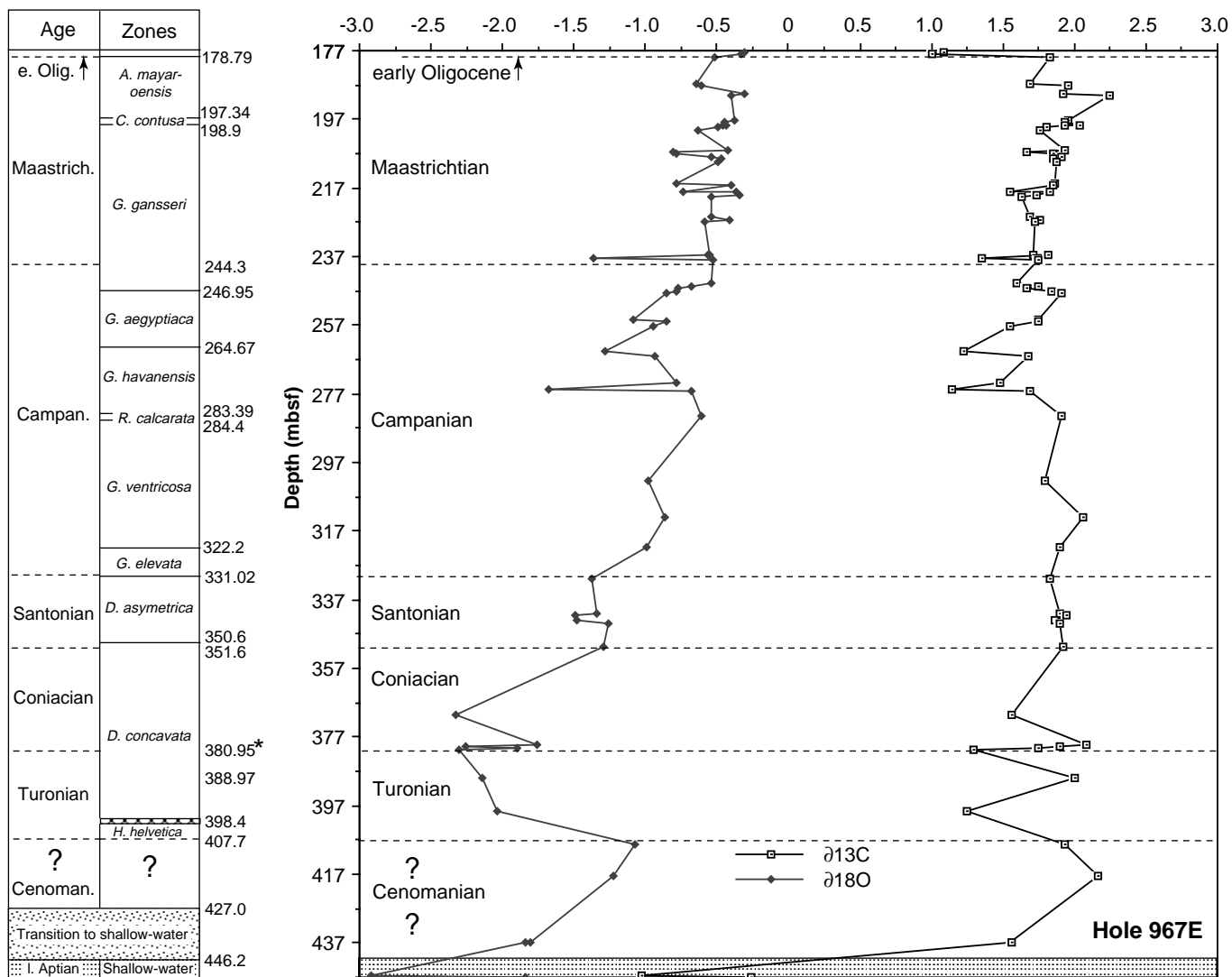


Figure 5. Oxygen and carbon isotope record ($\delta^{18}\text{O}$ and $\delta^{13}\text{C}$) of the Cretaceous sequence (Hole 967E) plotted vs. planktonic foraminiferal zones, age, and depth. Note: * at 380.95 mbsf = carbon isotope shift correlated to the Turonian/Coniacian boundary (see text section, "Cretaceous Isotope Stratigraphy," for explanation).

Table 5. Stable isotopes ($\delta^{13}\text{O}$ and $\delta^{13}\text{C}$) of Cretaceous bulk samples from Hole 967E.

Core, section, interval (cm)	Depth	$\delta^{13}\text{C}$	$\delta^{13}\text{O}$
160-967E-			
8R-1, 41-43	177.31	1.08	-0.302
8R-1, 92-94	177.82	1.005	-0.333
8R-2, 50-52	178.79	1.824	-0.519
9R-1, 3-8	186.53	1.69	-0.639
9R-1, 51-53	187.01	1.957	-0.612
9R-3, 57-59	189.5	1.916	-0.308
9R-3, 111-114	190.04	2.243	-0.403
10R-1, 114-117	197.34	1.961	-0.372
10R-2, 0-3	197.58	1.928	-0.45
10R-2, 98-100	198.56	2.038	-0.438
10R-3, 0-4	198.9	1.934	-0.454
10R-3, 60-62	199.5	1.81	-0.489
10R-3, 127-129	200.17	1.761	-0.628
11R-1, 4-6	205.84	1.93	-0.427
11R-1, 57-59	206.37	1.663	-0.802
11R-2, 38-40	207.21	1.855	-0.788
11R-3, 32-38	208.15	1.908	-0.544
11R-3, 82-84	208.65	1.846	-0.47
11R-CC, 33-35	209.28	1.873	-0.489
12R-1, 12-14	215.52	1.861	-0.788
12R-1, 72-74	216.12	1.846	-0.399
12R-2, 109-113	217.99	1.551	-0.738
12R-3, 0-3	218.16	1.828	-0.368
12R-3, 90-93	219.06	1.736	-0.348
12R-4, 11-15	219.61	1.626	-0.545
13R-1, 42-44	225.52	1.693	-0.541
13R-1, 107-108	226.17	1.754	-0.408
13R-2, 29-31	226.83	1.728	-0.584
14R-2, 26-35	236.46	1.717	-0.552
14R-2, 44-47	236.64	1.815	-0.564
14R-2, 109-123	237.29	1.35	-1.358
14R-3, 13-15	237.83	1.749	-0.523
15R-1, 24-26	244.54	1.598	-0.544
15R-1, 124-126	245.54	1.75	-0.677
15R-2, 31-34	246.04	1.667	-0.772
15R-2, 122-124	246.95	1.834	-0.785
15R-3, 20-24	247.43	1.908	-0.853
16R-1, 131-140	255.21	1.748	-1.08
16R-2, 32-40	255.72	1.743	-0.848
16R-3, 35-36	257.2	1.545	-0.949
17R-1, 117-120	264.67	1.227	-1.278
17R-2, 127-134	266.17	1.673	-0.938
18R-1, 89-90	273.99	1.476	0.786
18R-2, 113-114	275.51	1.148	-1.672
18R-3, 29-30	276.09	1.693	-0.681
19R-1, 69-71	283.39	1.909	-0.606
21R-1, 46-48	302.36	1.792	-0.982
21R-1, 113-116	312.73	2.059	-0.86
23R-2, 33-34	321.53	1.898	-0.991
24R-1, 22-23	331.02	1.828	-1.374
25R-1, 42-43	340.92	1.893	-1.346
25R-1, 116-117	341.66	1.942	-1.492
25R-2, 93-95	342.89	1.865	-1.483
25R-3, 65-67	344.08	1.897	-1.26
26R-1, 50-58	350.6	1.919	-1.296
28R-1, 107-110	370.37	1.562	-2.328
29R-1, 41-48	379.21	2.085	-1.755
29R-1, 100-102	379.8	1.903	-2.262
29R-2, 10-12	380.4	1.749	-1.896
29R-2, 65-67	380.95	1.298	-2.299
30R-1, 30-34	388.7	2.002	-2.141
31R-1, 4-10	398.44	1.246	-2.04
32R-1, 56-60	408.26	1.933	-1.074
33R-1, 6-12	417.46	2.162	-1.228
35R-1, 0-5	436.6	1.561	-1.838
36R-1, 10-16	446.3	-1.031	-2.919

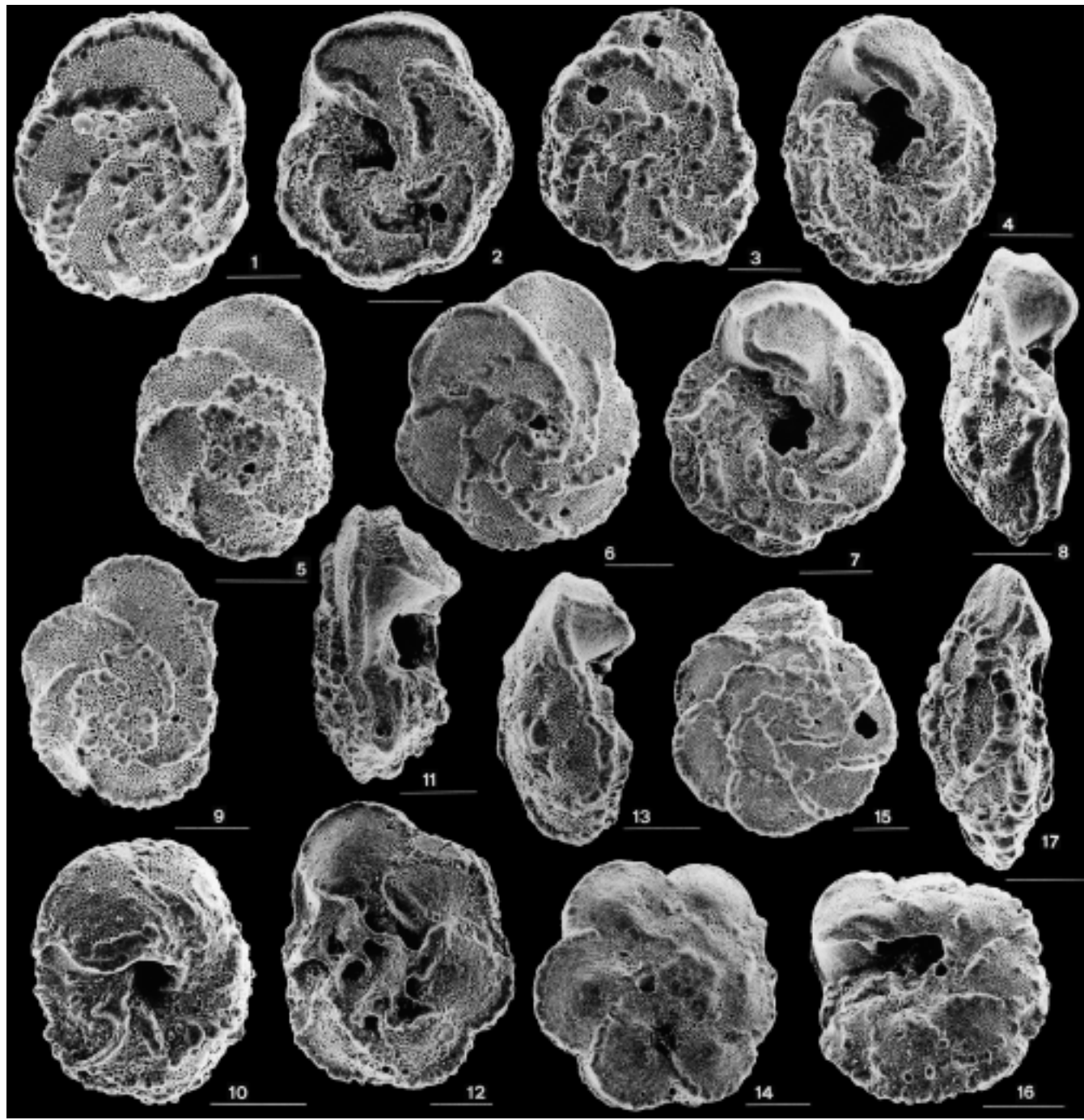


Plate 1. **1.** *Marginotruncana sinuosa*, spiral view. Sample 160-967E-26R-CC. **2.** *Marginotruncana sinuosa*, umbilical view. Sample 160-967E-26R-CC. **3.** *Marginotruncana coronata*, spiral view. Sample 160-967E-27R-CC. **4.** *Marginotruncana coronata*, umbilical view. Sample 160-967E-27R-CC. **5.** *Marginotruncana pseudolineana*, spiral view. Sample 160-967E-29R-2, 87–89 cm. **6.** *Globotruncana arca*, spiral view. Sample 160-967E-13R-CC. **7.** *Globotruncana arca*, umbilical view. Sample 160-967E-13R-CC. **8.** *Globotruncana arca*, side view. Sample 160-967E-13R-CC. **9.** *Globotruncana rosetta*, spiral view. Sample 160-967E-10R-CC. **10.** *Globotruncana rosetta*, umbilical view. Sample 160-967E-10R-CC. **11.** *Globotruncana ventricosa*, side view. Sample 160-967E-10R-CC. **12.** *Globotruncana ventricosa*, umbilical view. Sample 160-967E-10R-CC. **13.** *Globotruncana bulloides*, side view. Sample 160-967E-13R-CC. **14.** *Globotruncana bulloides*, spiral view. Sample 160-967E-13R-CC. **15.** *Globotruncana orientalis*, spiral view. Sample 160-967E-10R-CC. **16.** *Globotruncana orientalis*, umbilical view. Sample 160-967E-10R-CC. **17.** *Globotruncana orientalis*, side view. Sample 160-967E-10R-CC. All scale bars = 100 µm.

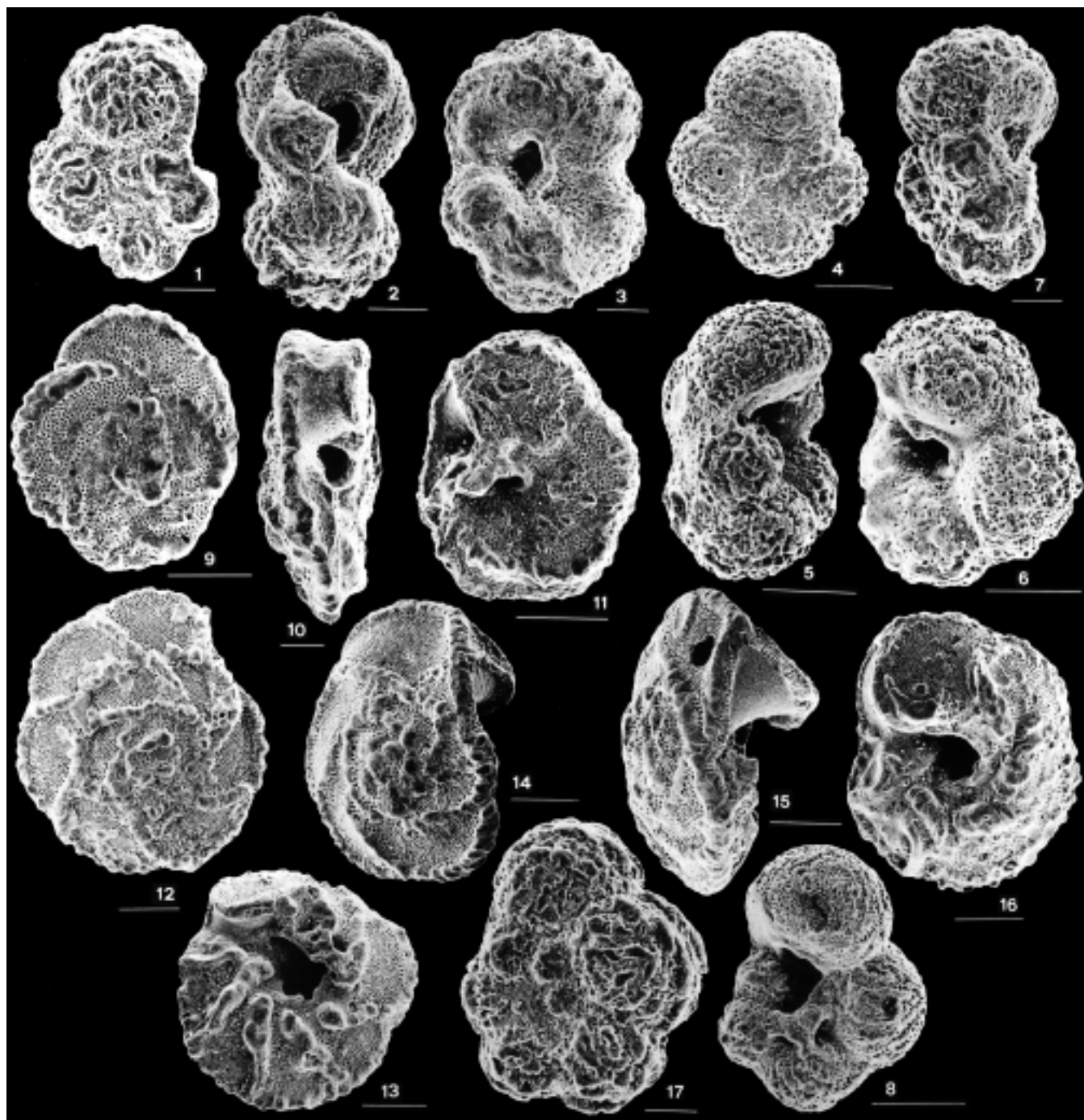


Plate 2. **1.** *Rugoglobigerina macrocephala*, spiral view. Sample 160-967E-13R-CC. Scale bar = 40 µm. **2.** *Rugoglobigerina macrocephala*, side view. Sample 160-967E-13R-CC. Scale bar = 40 µm. **3.** *Rugoglobigerina macrocephala*, umbilical view. Sample 160-967E-13R-CC. Scale bar = 40 µm. **4.** *Archaeoglobigerina blowi*, spiral view. Sample 160-967E-8R-CC. Scale bar = 100 µm. **5.** *Archaeoglobigerina blowi*, side view. Sample 160-967E-8R-CC. Scale bar = 100 µm. **6.** *Archaeoglobigerina blowi*, umbilical view. Sample 160-967E-8R-CC. Scale bar = 100 µm. **7.** *Rugoglobigerina rugosa*, side view. Sample 160-967E-13R-CC. Scale bar = 40 µm. **8.** *Rugoglobigerina rugosa*, umbilical view. Sample 160-967E-8R-CC. Scale bar = 100 µm. **9.** *Abathomphalus mayaroensis*, spiral view. Sample 160-967E-8R-CC. Scale bar = 100 µm. **10.** *Abathomphalus mayaroensis*, side view. Sample 160-967E-8R-CC. Scale bar = 40 µm. **11.** *Abathomphalus mayaroensis*, umbilical view. Sample 160-967E-8R-CC. Scale bar = 100 µm. **12.** *Globotruncana dupeublei*, spiral view. Sample 160-967E-10R-CC. Scale bar = 100 µm. **13.** *Globotruncana dupeublei*, umbilical view. Sample 160-967E-10R-CC. Scale bar = 100 µm. **14.** *Globotruncanita stuartiformis*, spiral view, slightly oblique. Sample 160-967E-10R-CC. Scale bar = 100 µm. **15.** *Globotruncanita stuartiformis*, side view. Sample 160-967E-10R-CC. Scale bar = 100 µm. **16.** *Globotruncanita stuartiformis*, umbilical view. Sample 160-967E-10R-CC. Scale bar = 100 µm. **17.** *Rugotruncana?* sp., spiral view. Sample 160-967E-13R-CC. Scale bar = 40 µm.

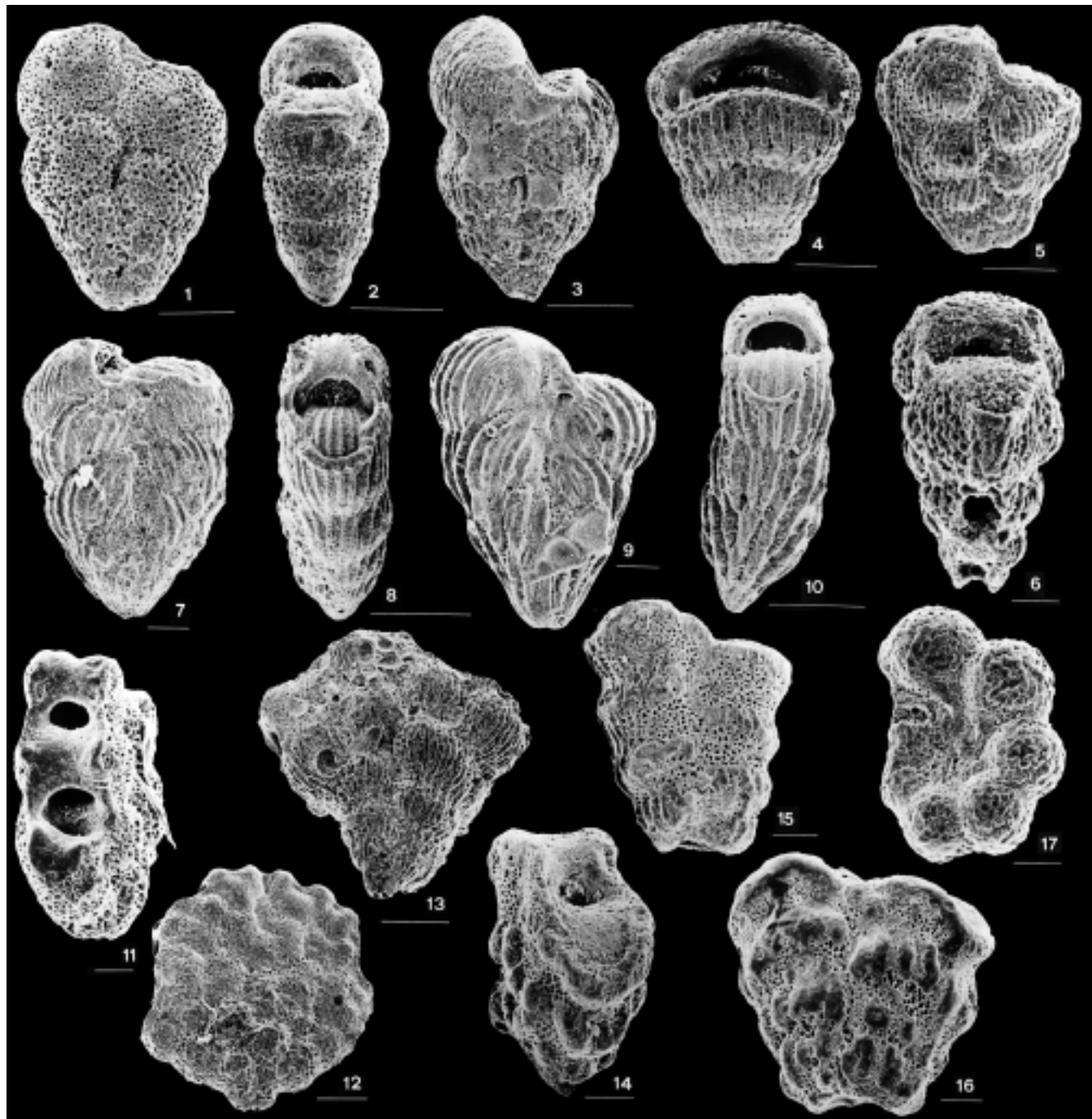


Plate 3. **1.** *Heterohelix punctulata*, side view. Sample 160-967E-10R-CC. Scale bar = 100 µm. **2.** *Heterohelix punctulata*, edge view. Sample 160-967E-10R-CC. Scale bar = 100 µm. **3.** *Pseudo-textularia elegans*, side view. Sample 160-967E-8R-CC. Scale bar = 100 µm. **4.** *Pseudotextularia elegans*, edge view. Sample 160-967E-8R-CC. Scale bar = 100 µm. **5.** *Heterohelix carinata*, side view. Sample 160-967E-26R-CC. Scale bar = 40 µm. **6.** *Heterohelix carinata*, edge view. Sample 160-967E-26R-CC. Scale bar = 20 µm. **7.** *Pseudoguembelina costulata*, side view. Sample 160-967E-8R-CC. Scale bar = 100 µm. **8.** *Pseudoguembelina costulata*, edge view. Sample 160-967E-8R-CC. Scale bar = 100 µm. **9.** *Pseudoguembelina excolata*, side view. Sample 160-967E-10R-CC. Scale bar = 40 µm. **10.** *Pseudoguembelina excolata*, edge view. Sample 160-967E-10R-CC. Scale bar = 100 µm. **11.** *Ventilabrella multicamerata*, apertural view. Sample 160-967E-10R-CC. Scale bar = 40 µm. **12.** *Ventilabrella multicamerata*, side view. Sample 160-967E-10R-CC. Scale bar = 100 µm. **13.** *Planoglobulina acervulinoides*, side view. Sample 160-967E-10R-CC. Scale bar = 100 µm. **14.** *Sigilia decoratissima carpatica*, apertural view. Sample 160-967E-26R-CC. Scale bar = 40 µm. **15.** *Sigilia decoratissima carpatica*, side view. Sample 160-967E-26R-CC. Scale bar = 40 µm. **16.** *Sigilia decoratissima carpatica*, side view. Sample 160-967E-26R-CC. Scale bar = 40 µm. **17.** *Globigerinelloides prairiehillensis*, umbilical view. Sample 160-967E-13R-CC. Scale bar = 40 µm.

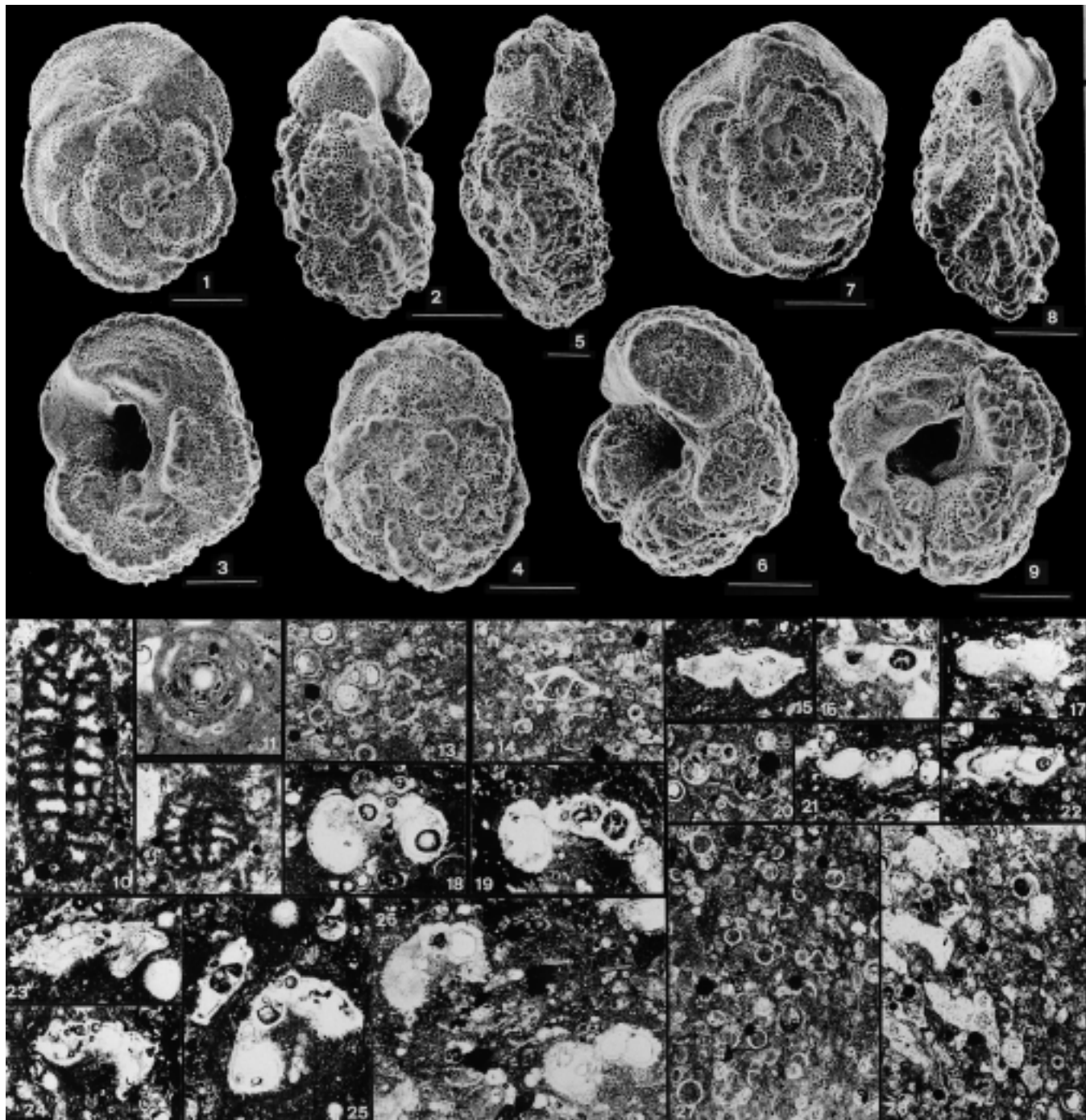


Plate 4. **1.** *Contusotruncana fornicata*, spiral view. Sample 160-967E-10R-CC. Scale bar = 100 µm. **2.** *Contusotruncana fornicata*, side view. Sample 160-967E-10R-CC. Scale bar = 100 µm. **3.** *Contusotruncana fornicata*, umbilical view. Sample 160-967E-10R-CC. Scale bar = 100 µm. **4.** *Contusotruncana plummerae*, spiral view. Sample 160-967E-19R-1, 69–71 cm. Scale bar = 100 µm. **5.** *Contusotruncana plummerae*. Scale bar = 40 µm. **6.** *Contusotruncana plummerae*, umbilical view. Sample 160-967E-10R-CC. Scale bar = 100 µm. **7.** *Contusotruncana patelliformis*, spiral view. Sample 160-967E-10R-CC. Scale bar = 100 µm. **8.** *Contusotruncana patelliformis*, side view. Sample 160-967E-10R-CC. Scale bar = 100 µm. **9.** *Contusotruncana patelliformis*, umbilical view. Sample 160-967E-10R-CC. Scale bar = 100 µm. **10.** *Cuneolina* sp., transversal view. Sample 160-967E-35R-1, 2–5 cm, 55×. **11.** *Archaealveolina reicheli*, equatorial view. Sample 160-967E-41R-1, 2–5 cm, 80×. **12.** *Archaealveolina reicheli*, tangential view. Sample 160-967E-41R-1, 2–5 cm, 55×. **13.** *Favusella washitensis*, axial view. Sample 160-967E-32R-1, 56–60 cm, 55×. **14.** *Rotalipora* sp., not centered axial view. Sample 160-967E-33R-1, 7–10 cm, 55×. **15.** *Dicarinella primitiva*, axial view. Sample 160-967E-30R-1, 15–20 cm, 55×. **16.** *Dicarinella primitiva*, axial view. Sample 160-967E-30R-1, 30–34 cm, 55×. **17.** *Dicarinella* sp., axial view. Sample 160-967E-30R-1, 30–34 cm, 55×. **18.** *Whiteinella baltica*, axial view. Sample 160-967E-30R-1, 15–20 cm, 55×. **19.** *Whiteinella aprica*, axial view. Sample 160-967E-30R-1, 30–34 cm, 55×. **20.** *Hedbergella delicensis*, axial view. Sample 160-967E-32R-1, 56–60 cm, 55×. **21.** *Hedbergella flandriini*, axial view. Sample 160-967E-30R-1, 30–34 cm, 55×. **22.** *Dicarinella* sp., axial view. Sample 160-967E-30R-1, 30–34 cm, 55×. **23.** *Marginotruncana sigali* group, axial view. Sample 160-967E-30R-1, 15–20 cm, 55×. **24.** *MARGINOTRUNCANA* sp. aff. *M. marianosi*, axial view. Sample 160-967E-30R-1, 30–34 cm, 55×. **25.** *Praeglobotruncana gibba* (right) and *Dicarinella canaliculata* (above left), both axial views. Sample 160-967E-30R-1, 15–20 cm, 55×. **26.** Two specimens of *Whiteinella* sp., oblique views. Sample 160-967E-30R-1, 30–34 cm, 55×. **27.** Calcispheres. Sample 160-967E-33R-1, 7–10 cm, 60×. **28.** Calcispheres and echinoid fragments. Sample 160-967E-32R-1, 12–14 cm, 60×.